University of Kentucky
UKnowledge

Theses and Dissertations--Pharmacy College of Pharmacy

2023

Investigation of Folate-Poly(Glutamic Acid)/Polyethylenimine/ DNA Complexes for in vitro Gene Delivery

Caleb Akers
University of Kentucky, caleb.akers@uky.edu
Author ORCID Identifier:
https://orcid.org/0000-0001-9288-3303
Digital Object Identifier: https://doi.org/10.13023/etd.2023.383

Right click to open a feedback form in a new tab to let us know how this document benefits you.

Recommended Citation

Akers, Caleb, "Investigation of Folate-Poly(Glutamic Acid)/Polyethylenimine/DNA Complexes for in vitro Gene Delivery" (2023). *Theses and Dissertations--Pharmacy*. 155.
https://uknowledge.uky.edu/pharmacy_etds/155

This Doctoral Dissertation is brought to you for free and open access by the College of Pharmacy at UKnowledge. It has been accepted for inclusion in Theses and Dissertations--Pharmacy by an authorized administrator of UKnowledge. For more information, please contact UKnowledge@lsv.uky.edu.

STUDENT AGREEMENT:

I represent that my thesis or dissertation and abstract are my original work. Proper attribution has been given to all outside sources. I understand that I am solely responsible for obtaining any needed copyright permissions. I have obtained needed written permission statement(s) from the owner(s) of each third-party copyrighted matter to be included in my work, allowing electronic distribution (if such use is not permitted by the fair use doctrine) which will be submitted to UKnowledge as Additional File.

I hereby grant to The University of Kentucky and its agents the irrevocable, non-exclusive, and royalty-free license to archive and make accessible my work in whole or in part in all forms of media, now or hereafter known. I agree that the document mentioned above may be made available immediately for worldwide access unless an embargo applies.

I retain all other ownership rights to the copyright of my work. I also retain the right to use in future works (such as articles or books) all or part of my work. I understand that I am free to register the copyright to my work.

REVIEW, APPROVAL AND ACCEPTANCE

The document mentioned above has been reviewed and accepted by the student's advisor, on behalf of the advisory committee, and by the Director of Graduate Studies (DGS), on behalf of the program; we verify that this is the final, approved version of the student's thesis including all changes required by the advisory committee. The undersigned agree to abide by the statements above.

Caleb Akers, Student

Dr. Daniel Pack, Major Professor

Dr. David Feola, Director of Graduate Studies

INVESTIGATION OF FOLATE-POLY(GLUTAMIC ACID)/POLYETHYLENIMINE/DNA COMPLEXES FOR IN VITRO GENE DELIVERY

DISSERTATION

A dissertation submitted in partial fulfillment of the
requirements for the degree of Doctor of Philosophy in the
College of Pharmacy
at the University of Kentucky

By
Caleb Michael Akers
Lexington, Kentucky
Director: Dr. Daniel W Pack, Professor of Chemical & Materials Engineering and Pharmaceutical Sciences
Lexington, Kentucky
2023

Copyright © Caleb Michael Akers 2023
https://orcid.org/0000-0001-9288-3303

ABSTRACT OF DISSERTATION

INVESTIGATION OF FOLATE-POLY(GLUTAMIC ACID)/POLYETHYLENIMINE/DNA COMPLEXES FOR IN VITRO GENE DELIVERY

Gene therapy is currently being studied as a treatment for a variety of indications, including cancer, infectious disease, and cardiovascular diseases, among others. While many of the early treatments in the field involved the use of viral delivery methods, various safety, ethical, and financial concerns limit the potential uses of this methodology. As such, more recent research has focused on developing non-viral delivery platforms to alleviate some of the issues inherent in viral delivery. Recently, the release of the COVID-19 vaccines from Pfizer and Moderna represents a promising use of non-viral delivery as both utilized a lipid-based delivery vector.

Despite the ease of production and adaptability of recent non-viral platforms, these vectors suffer when compared to their viral counterparts in terms of delivery efficiency. This is due to the various biological barriers facing any gene delivery method. While viruses have had millennia to evolve and adapt to these barriers, non-viral vectors still face issues with circulation times, gene encapsulation, cell-surface interactions, internalization, endosomal escape, intracellular trafficking, and nuclear release of the

gene payload. Previous research has revealed that the surface charge of certain delivery vectors can affect various of the aforementioned barriers. To further improve upon the knowledge of charge effects, the following thesis outlines the effects of adding folate receptor-targeting to negative polyplexes.

Chapter 1 provides background information on various gene delivery vehicles and folic acid. Chapter 2 begins with the generation and characterization of a folate-tagged polymer for use in generating ternary polyplexes for gene delivery. Early studies utilizing this targeting method show folate tag concentration affects overall gene delivery efficiency, with a lower tag ratio outperforming the highest folate concentration. Chapter 3 then moves on to investigate the effect of folate receptor-targeting on internalization pathway. In a folate receptor-positive cell line, the folate-tagged polyplexes are shown to divert particles down the expected caveolar endocytic pathway, while folate receptor-negative cells show non-specific uptake of particles. Chapter 4 explains an investigation into the intracellular trafficking effects of folate-tagged polyplexes. Both folate receptor-positive and -negative cell lines show strong reliance on an active transport pathway within the cell to reach the nucleus. Finally, chapter 5 includes a prospective on future directions for both this continued project as well as non-viral vectors as a platform.

The goal of this work was to expand upon the benefits of negatively charged ternary polyplexes by utilizing a targeting methodology to improve overall delivery efficiency of the resulting particles. The evolution and continued adaptation of non-viral vectors will be key to developing a true competitor to viral gene delivery. Future improvements upon this platform will include incorporation of immune-shielding

methodologies or the alteration of the ligand linkage to generate a potentially improved targeting effect.

KEYWORDS: Polymeric Gene Delivery, Folic Acid, Gene Therapy, Endocytosis, Cancer

Caleb Michael Akers

(Name of Student)

01/28/2023

Date

INVESTIGATION OF FOLATE-POLY(GLUTAMIC ACID)/POLYETHYLENIMINE/DNA COMPLEXES FOR IN VITRO GENE DELIVERY

By

Caleb Michael Akers

Dr. Daniel W. Pack

Director of Dissertation

Dr. David Feola

Director of Graduate Studies

01/28/2023

Date

ACKNOWLEDGMENTS

The successful preparation of this dissertation could not have been completed without the aid of many individuals. I would first like to thank my family and friends for their constant support in all of my years at UK, especially my lovely wife, who has made every long day and difficult experience so much better. My parents have been amazing supports and cheerleaders, without which I could not have succeeded. I give many thanks to my friends, for their regular morale boosts and encouragement to keep going.

I could not have reached this point without significant academic encouragement and guidance. For this, I would like express my appreciation and gratitude to my Dissertation Chair, Dr. Daniel Pack, as well as the remainder of my advisory committee, Dr. Tom Dziubla, Dr. Vincent Venditto, and Dr. Younsoo Bae. I'd also like to thank Dr. David Rodgers for taking the time out of his day to serve as my outside examiner for this thesis defense. Similarly, for their guidance and encouragement, I would like to thank my lab mates, Dr. Landon Mott, Dr. Logan Warriner, and Levi Lampe alongside my colleagues, Dr. David Nardo, Dr. Preye Agbana, and Daniel Kolpek.

Lastly, I would like to thank Dr. Gosia Chwatko for acquiring the GPC chromatograms and Dr. Vivekanandan Subramanian for gathering the NMR spectra.

TABLE OF CONTENTS

ACKNOWLEDGMENTS iii

LIST OF TABLES vii

LIST OF FIGURES viii

Introduction and Background 1

1.1 Introduction 1

1.2 Barriers to Gene Therapy 1

1.3 Current Gene Therapy Methods 5

1.3.1 Naked Plasmid Delivery 5

1.3.2 Viral Gene Delivery 6

1.4 Characteristics of Anionic Polyplexes 12

1.4.1 Circulation Improvements 14

1.4.2 Lowered Cell Uptake 14

1.4.3 Cytotoxicity Improvements 15

1.5 Folic Acid-Related Therapeutics 16

1.6 Concluding Remarks 17

CHAPTER 2. Development of Folate-Receptor Targeted Ternary Polyplex for Gene Delivery 18

2.1 Introduction 18

2.2 Materials and Methods 20

2.2.1 Cell Culture 20

2.2.2 Materials 20

2.2.3 Synthesis of Folic Acid-PGA Conjugate 21

2.2.4 Verification of Folic Acid conjugation 21

2.2.5 NMR 22

2.2.6 Gel Permeation Chromatography 23

2.2.7 Polyplex Formation 23

2.2.8 Size and Zeta Potential 24

2.2.9 Polyplex Transfection 24
2.3 Results and Discussion 25
2.3.1 PGA-Fol Synthesis and Conjugation Ratio Confirmation 25
2.3.2 Chemical Structure Elucidation through Nuclear Magnetic Resonance 26
2.3.3 Crosslinking Determination through Gel Permeation Chromatography 31
2.3.4 Determining the Physicochemical Characteristics of Ternary PGA/PEI/DNA Polyplexes 32
2.3.5 Folate-Receptor Targeting Viability as Determined by Transfection 34
2.4 Conclusions 36

CHAPTER 3. INVESTIGATION OF FOLATE RECEPTOR-TARGETING EFFECTS ON ENDOCYTIC UPTAKE PATHWAY 38
3.1 Introduction 38
3.2 Materials and Methods 41
3.2.1 Cell Culture 41
3.2.2 Materials 41
3.2.3 Polyplex Formation 42
3.2.4 Transfection in the Presence of Endocytic Inhibitors 42
3.2.5 Polyplex Uptake in the Presence of Endocytic Inhibitors 43
3.2.6 siRNA Knockdown 44
3.3 Results and Discussion 44
3.3.1 Transfection Efficiency of Folate Receptor-Targeted Particles Relies on Caveolin and Lipid Raft-Dependent Pathways 44
3.3.2 Polyplex Uptake Effects of Folate Receptor Targeting 48
3.3.3 siRNA Knockdown Indicates Reliance on Lipid Raft Endocytic Pathway 50
3.4 Conclusions 52

CHAPTER 4. INVESTIGATION OF FOLATE RECEPTOR-TARGETING EFFECTS ON INTRACELLULAR TRAFFICKING 56
4.1 Introduction 56
4.2 Materials and Methods 58
4.2.1 Cell Culture 58
4.2.2 Materials 58

4.2.3 Polyplex formation 59
4.2.4 Intracellular Inhibitor Toxicity 59
4.2.5 Transfection in the Presence of Intracellular Trafficking Inhibitors 60
4.2.6 Polyplex Uptake in the Presence of Intracellular Trafficking Inhibitors 61
4.3 Results and Discussion 62
4.3.1 Intracellular Inhibitor Toxicity 62
4.3.2 Reliance on Active Pathways for Transfection 65
4.3.3 Polyplex Uptake Investigation through Flow Cytometry 66
4.4 Conclusions 68
CHAPTER 5. PERSPECTIVES AND FUTURE DIRECTIONS 70
APPENDIX 74
LIST OF REFERENCES 90
CALEB AKERS VITA 95

LIST OF TABLES

Table 1 Summary table of endocytic inhibitors…….46
Table 2 Summary table of intracellular inhibitors…….60

LIST OF FIGURES

Figure 1 Schematic of endocytic pathways of entry and subsequent intracellular trafficking 3
Figure 2 Selected Lipid Structures 9
Figure 3 Selected Polymer Structures 11
Figure 4 Ternary Polyplex Formation Schematic 13
Figure 5 Chemistry scheme for the conjugation of folic acid to PGA through a PEG600 linker. 26
Figure 6 Proton NMR Spectra for the poly-L-α-glutamic acid starting material with peak identification 27
Figure 7 Proton NMR of Folate-PEG600-NH_2 starting material with peak identification 28
Figure 8 Proton NMR spectra and structure for PGA-Fol(1) with peak identification 29
Figure 9 Proton NMR spectra and structure for PGA-Fol(3) with peak identification 30
Figure 10 Proton NMR and structure for PGA-Fol(7) with peak identification 31
Figure 11 GPC chromatogram of PGA and PGA-Fol samples 32
Figure 12 Dynamic Light Scattering and Zeta potential of a range of polyplex compositions and folate tag ratios. All polplexes formed at an X:3:1 PGA/PEI/DNA weight ratio.Error bars represent standard deviation 34
Figure 13 Targeted anionic polyplex transfection using various folic acid tagging ratios in both HeLa and HEK 293 cell lines. Particles were prepared at a 5.2:3:1 (PGA-Fol/PEI/DNA) weight ratio and incubated with cells in the presence of serum. (n=6, error bars represent standard error, *p<0.05) 36
Figure 14 HeLa (left) and HEK 293 (right) cells were transfected with ternary polyplexes tagged with 1, 3, or 7 folates per PGA chain. Luciferase signal expresses gene delivery efficiency and all samples are normalized to non-inhibited controls (n=6, error bars represent standard error, *p<0.05 compared to non-inhibited cells) 47
Figure 15 HeLa (left) and HEK 293 (right) transfected with YOYO-1 labeled polyplexes for flow cytometry measurement of particle uptake. All samples normalized to non-inhibited controls (n=3, error bars represent standard deviation, *p<0.05 compared to non-inhibited cells) 50
Figure 16 HeLa (left) and HEK 293 (right) cells were transfected with anionic polyplexes after specified endocytic pathways were knockdown via siRNA. (n=6, error bars represent standard error, *p<0.05 compared to cells which weren't knocked down) 52
Figure 17 Pathway Summary for Targeted and non-Targeted Polyplexes 54
Figure 18 Intracellular Inhibitor Toxicity in HeLa cells. Concentration at 80% cell viability was taken for further polyplex experiments. (n=4) 63
Figure 19 Intracellular Inhibitor Toxicity in HEK 293 cells. Concentration at 80% cell viability taken for further polyplex experiments. (n=4) 64
Figure 20 HeLa (left) and HEK 293 (right) were transfected with ternary anionic polyplexes in the presence and absence of various small molecule intracellular trafficking inhibitors. Luciferase expression is used as a measure of gene delivery efficiency. (n=6, error bars represent standard error, *p<0.05 compared to non-inhibited cells) 66

Figure 21 HeLa (left) and HEK 293 (right) were transfected with ternary anionic polyplexes tagged with a YOYO-1 DNA label in the presence and absence of various small molecule intracellular trafficking inhibitors. Mean fluorescence is used as a measure of particle uptake (n=3, error bars represent standard deviation, *$p<0.05$ compared to non-inhibited cells) 68
Figure 22: ^{13}C spectra for PGA (32 scans) 75
Figure 23: HSQC spectra for PGA (32 scans) 76
Figure 24: ^{13}C spectra for Folate-PEG600-NH_2 (2000 scans) 77
Figure 25: COSY spectra for Folate-PEG600-NH_2 (8 scans) 78
Figure 26: HSQC spectra for Folate-PEG600-NH_2 (8 scans) 78
Figure 27: ^{15}N HSQC spectra for Folate-PEG600-NH_2 (16 scans) 79
Figure 28: NOESY spectra for Folate-PEG600-NH_2 (16 scans) 79
Figure 29: TOCSY spectra for Folate-PEG600-NH_2 (16 scans) 80
Figure 30: HSQC for PGA-Fol(1) (16 scans) 82
Figure 31: ^{15}N HSQC for PGA-Fol(1) (32 scans) 82
Figure 32: HSQC for PGA-Fol(3) (64 scans) 85
Figure 33: ^{15}N HSQC for PGA-Fol(3) (128 scans) 85
Figure 34: HSQC for PGA-Fol(7) (16 scans) 88
Figure 35: ^{15}N HSQC for PGA-Fol(7) (64 scans) 88

INTRODUCTION AND BACKGROUND

1.1 Introduction

This chapter will cover a basic explanation of gene therapy and delivery through an introductory history of the field as well as current delivery vectors being investigated. Benefits and downsides of each explored vector are also conveyed as there currently exists no one-size-fits-all solution to the barriers facing gene delivery. An interesting targeting moiety, folic acid, is also explored as a potential improvement upon some of the non-viral vectors mentioned previously. Finally, the exploration of a new generation of polymeric gene delivery vectors, ternary anionic polyplexes, is explained through its various benefits and hinderances in the field of gene delivery.

1.2 Barriers to Gene Therapy

The field of gene therapy is based around the principle that human disease can be treated through the introduction of external genetic material into the patient's cells [1]. Generally speaking, the genetic material introduced falls under three functional categories: the addition of function, the loss of function, or cell death. The addition of function can be accomplished through the delivery of extra copies of a gene needed to produce a desired product. An example of this could be incorporating genes necessary for the production of insulin in the cells of a diabetic patient [2]. In the second case, one can reduce the production of mutant huntingtin protein in patients with Huntington's disease [3]. Finally, especially in the case of cancer, simply causing cell death through the delivery of a suicide gene presents a currently researched use of gene therapy [4].

The first reported clinical trial using gene therapy began in 1990 for the treatment of severe combined immunodeficiency, or SCID [5]. This first trial opened the door for many other gene therapies and delivery methodologies to emerge. There have since been over 4000 clinical trials worldwide utilizing gene therapy for numerous other indications [6], with a particular focus on cancer therapies. Despite the decades of research since Blaese et al.'s first trial and thousands of approved clinical trials since, there exist only 27 FDA-approved cell and gene therapies [7]. The lack of success in these trials, while disappointing, provides exciting avenues to explore the various barriers to a successful gene therapy.

Any gene therapy system faces numerous barriers to successful delivery before even reaching the cell surface. A successful gene delivery vehicle must be able to condense and protect the genetic material both in solution and throughout circulation to its destination while also being able to release the gene where appropriate in the cell. This ideal vehicle should avoid agglomeration with serum proteins in circulation, which can lead to immunogenicity and degradation of the delivery vehicle. Targeted therapies are also of great benefit to avoid off-target localization of the gene payload which, at best, can lead to a lack of benefit from the treatment. Finally, a clinically successful product should be easy and inexpensive to produce, easy to administer, and remain stable over a reasonable shelf-life. All of these criteria for success only cover the barriers before reaching the cell of interest [1].

Following all of these barriers, the delivery vehicle must have a mechanism to enter the cell, often through some form of endocytosis. Endocytosis, in a broad sense, is

an internalization strategy in which external materials are engulfed by a segment of the cell membrane to be brought into the cell. The three best understood subsets of endocytosis include clathrin-mediated endocytosis, caveolar endocytosis, and macropinocytosis [8].

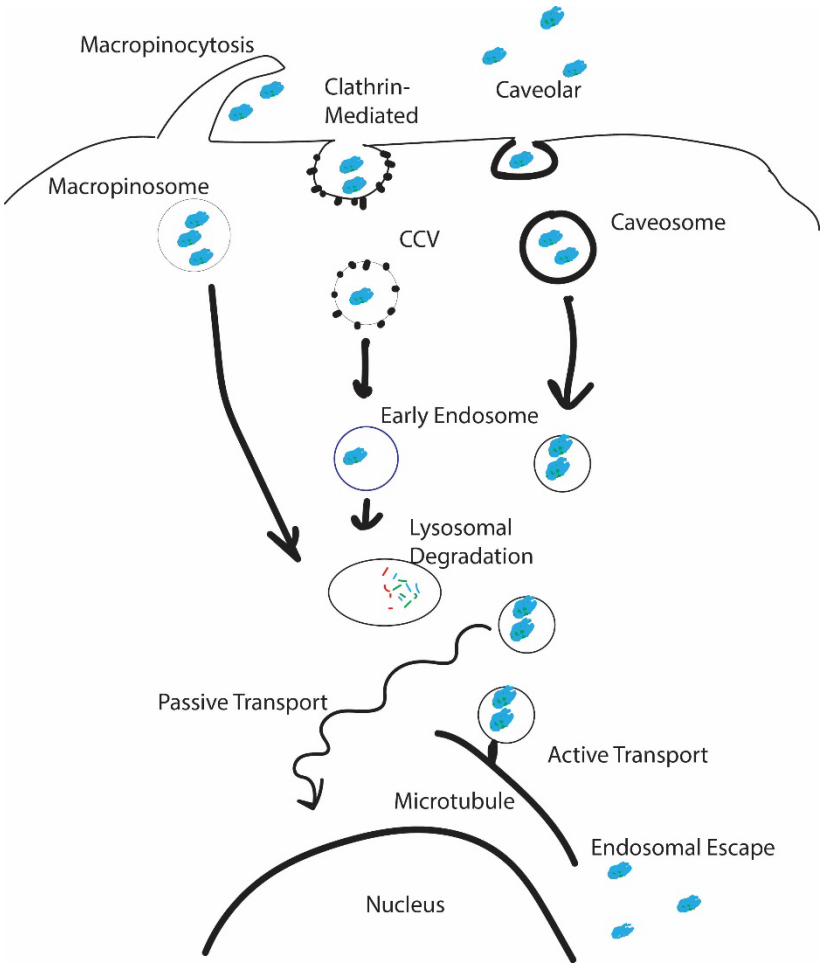

Figure 1 Schematic of endocytic pathways of entry and subsequent intracellular trafficking

Clathrin-mediated endocytosis, as the name suggests, relies on the accumulation of clathrin on the cell surface to form invaginations, called clathrin-coated pits. These pits then pinch off into the cell with the aid of dynamin to form a clathrin-coated vesicle (CCV), which ranges in size from 100-200 nm [9, 10]. The vesicle then acidifies to

around pH 6 as proton pumps transport hydrogen ions into the vesicle [8]. The CCV then progresses to a late endosome where pH approaches 5, eventually leading to lysosomal fusion for degradation of the endosomal cargo [10]. Generally, lysosomal degradation is accomplished through a combination of hydrolytic and proteolytic enzymes along with pH-related degradation [11]. This lysosomal degradation can be a significant hinderance to any delivery method that cannot escape the endosome before this stage.

Caveolar endocytosis is marked by the membrane protein, caveolin. Caveolin vesicles, or caveosomes, are flask-shaped invaginations around 120 nm in size [9]. This size measurement only covers physiological use though, as particles in the range of 500 nm have been shown to primarily enter the cell through a caveolin-mediated pathway [12]. Caveosomes lack the acidification and lysosomal trafficking processes involved in clathrin-mediated endocytosis, making this pathway more efficient for gene delivery vectors [13].

Macropinocytosis involves actin-driven membrane ruffling and subsequent large-scale engulfing of fluid and surrounding materials through a protrusion of the cell membrane. The completed, irregularly shaped vesicle, termed a macropinosome, can reach sizes into the micron range [8, 9, 13]. These vesicles are known to acidify and fuse with lysosomes for degradation similar to clathrin-associated pathways [14]. While this pathway is efficient at endocytosing large volumes of fluid and surrounding delivery vectors, the lysosomal degradative pathway and general lack of specificity make it a poor target for gene delivery.

Regardless of the preferred method of entry, the delivery vehicle must maintain protection of the genetic material while escaping the endosome. The delivery vector must then avoid lysosomal degradation, travel to the nucleus, and release the genetic material for transport into the nucleus. Each of these steps presents another potential point of failure for any potential delivery vehicle [1].

1.3 Current Gene Therapy Methods

1.3.1 Naked Plasmid Delivery

Approximately 13% of gene therapy clinical trials have centered around naked DNA delivery [6], or a plasmid delivered without any delivery vehicle or protective surrounding layer. These therapies are often utilized as vaccines as the naked DNA is taken up largely by muscle cells and leads to immune response to encoded antigens [15]. While intravenous delivery is poor for this form of delivery, as circulating nucleases will degrade free DNA, the simplicity of this treatment for vaccination has led to multiple human trials. Typical vaccination platforms utilize dead viruses, associated viral subunits, or attenuated live viruses to generate an immune response to the specific antigens found on the viral capsid. This strategy, while effective, presents safety concerns inherent to viral treatments which will be explained in the next section. Naked DNA vaccines alleviate some of these safety concerns. A second generation of these DNA vaccines seeks to improve upon the first by including additional plasmids encoding for adjuvants, meant to boost immune response, and broader-spectrum antigens to direct broader and heightened immune response [15]. Additional improvements for these vaccines come in

the form of needle-free delivery strategies and delivery vehicles to improve circulation viability.

1.3.2 Viral Gene Delivery

Viral delivery constitutes over 50% of gene therapy clinical trials [6] and with good reason. Viruses, as pathogens, have had millennia to develop a near-perfect system for gene delivery and ultimately their continued existence [16]. Compared to the mere decades of research into non-viral delivery, viruses are understandably the peak of gene delivery. Generally speaking, viral vectors comprise a nucleic acid genome packed in a protein capsid. Viruses are then classified by the type of nucleic acid genome contained, the composition of the capsid, and the presence or absence of an additional lipid coating on the outside of the capsid [17]. The nucleic acid genome falls under three categories: single stranded RNA, double stranded DNA, or single stranded DNA. The viral capsid containing this genome also aids in binding to the host cell and enabling entry into the cell [18]. The most relevant viruses for gene therapy are retroviruses, adenoviruses, adeno-associated viruses, and lentiviruses.

Retroviruses are among the oldest researched viral subsets for gene delivery. Retroviruses are utilized in the field of gene delivery due to their capacity to integrate their genome into the host's genetic material [18]. This allows for potentially lifelong alteration of the host cell and continued support of the therapeutic gene introduced. Retroviruses have also been shown to avoid producing immunogenic viral proteins. Unfortunately, retroviruses are hindered by their relatively small viral genome [19], limiting the size of gene they can introduce into a host cell. Also, while retroviruses can

integrate their genetic material into the host genome, issues arise in the host cell as the retroviral genome is inserted at random locations into the host [18]. This can disrupt the natural function of the cell and lead to lack of viability in the host system. Finally, retroviral vectors have only been shown to transduce dividing cells, hindering their use in certain disease states.

The plurality of clinical trials utilize adenoviruses to deliver their genetic cargo. Adenoviral vectors benefit from the ability to infect a wide variety of cell types, including those that are not actively dividing [18]. While the adenovirus does not integrate its genome into the host's, thus alleviating the issue of random insertion, this also means that an adenoviral treatment would be expected to require multiple administrations as the viral gene expression is only transient. Hindering the adenovirus further is the fact that viral proteins are also expressed in transduced cells, leading to immune response, further shortening the duration of therapeutic effect, generally lasting only 1-3 weeks on average [20]. Similarly to retroviruses, adenoviruses also have relatively small genomic capacity, limiting the types of treatments available for this system. This limited duration of treatment is of little hinderance, though, in the case of cancer, where delivery of a suicide gene need only be transient.

Adeno-associated viruses (AAVs) are small, single-stranded DNA viruses which, similar to adenoviruses, can infect both dividing and non-diving cells. Certain AAV serotypes have been shown to even cross the blood-brain barrier, a particularly difficult task for any delivery platform [21]. AAVs have been shown to integrate into the host genome at multiple chromosomal sites or remain extrachromosomal. AAV integration is found to be preferential toward Rep-binding sites on chromosome 19, 5 and 3 [22].

Additionally, AAVs lack a strong immune response, alleviating some safety concerns from the use of viral particles. However, humans have pre-existing antibodies to some AAV serotypes, limiting effectiveness of treatments utilizing this platform [23].

Finally, lentiviruses were developed from the human immunodeficiency virus (HIV) to become self-inactivating delivery vectors and have seen clinical use for the generation of CAR T-cell cancer therapies [24]. Lentiviruses, similar to the previous two examples, have the capability to infect both dividing and non-dividing cell types. Lentiviral vectors also integrate their genome into that of the host and avoid production of viral proteins to limit immune response. Unfortunately, this integration remains random, continuing the issue of mutagenesis in infected cells. Lentiviral development does show a strong step forward in the generation of further improved viral vectors for the treatment of future human diseases.

1.3.3 Non-Viral Gene Delivery

Non-viral gene delivery vectors generally fall under two categories: lipid and polymeric vectors. Non-viral therapies benefit over viral therapies in terms of production cost and time, versatility, as well as safety. Both lipid and polymeric vectors are capable of a wide range of facile alterations to their chemistry to allow for any number of delivery improvements, including cell-specific targeting, endosomal escape moieties, and immune system avoidance. Non-viral platforms also have a much wider range of deliverable genome sizes as they are more flexible in their composition compared to the relatively small capsid volume of viruses. In general, non-viral vectors still suffer in terms of

delivery efficiency when compared to viruses and can still lead to cytotoxicity in transfected cells [25].

The first generation of these non-viral vectors centered around the electrostatic binding of cationic lipids or polymers to the anionic phosphate backbone of nucleic acids. Termed lipoplexes and polyplexes, respectively, these initial binary complexes were developed to address the continuing problems and ethical concerns with viral vectors. The first reported lipoplex, utilizing the synthetic lipid DOTMA (1,2-di-O-octadecenyl-3-trimethylammonium propane), found great success in initial experiments with transfection efficiency [26]. Since this first lipoplex formulation, Lipofectamine, a combination mixture of DOSPA and DOPE, has become a gold-standard in lipid-based gene delivery [27, 28]. These lipoplexes and other similar compositions suffer from cytotoxicity in some cell types due to their high positive surface charge [1].

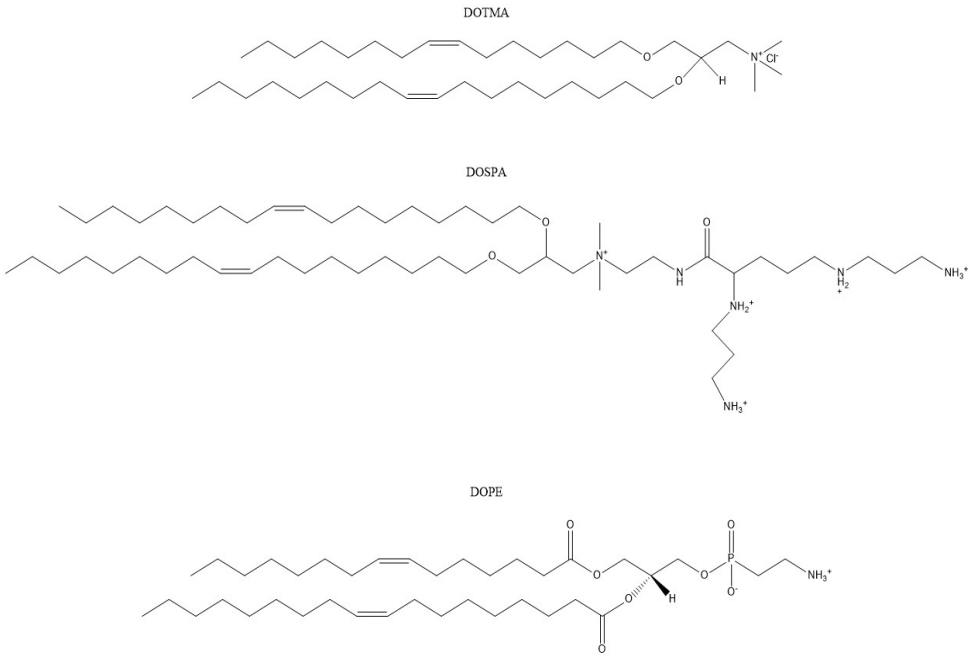

Figure 2 Selected Lipid Structures

Early polyplexes utilizing readily available cationic polymers largely utilized a high density of positive amines to compact nucleic acids into polyplexes. One of the most prevalent of these cationic polymers for gene delivery is polyethylenimine (PEI) [29, 30] . Branched PEI has shown improved gene delivery efficiency due to its effective endosomal escape mechanism, a so-called “proton sponge” effect [31]. The proton-sponge effect is a proposed hypothesis for the effectiveness of PEI stating that the prevalence of protonatable nitrogens allows PEI to accept the influx of protons without appreciably increasing the acidity in the endosomal environment. The concomitant influx of counterions causes osmotic swelling of the endosome and subsequent rupture, allowing for the release of the delivery vehicle into the cytosol. PEI suffers on its own due to significant cytotoxicity attributed to its high positive surface charge and ability to disrupt

biological membranes [32].

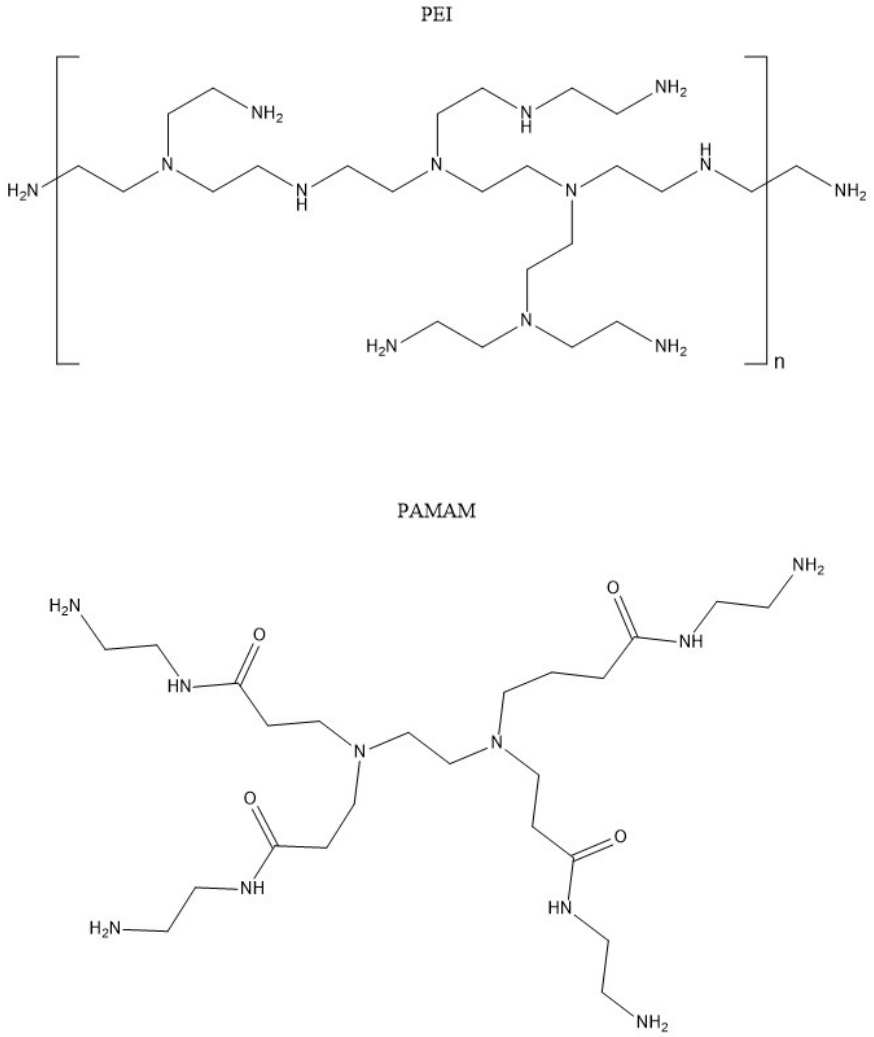

Figure 3 Selected Polymer Structures

A similarly amine-rich polymeric dendrimer, polyamidoamine (PAMAM), has been utilized in binary complexes as well for its high concentration of amine groups [33]. PAMAM synthesis is accomplished by the addition of repeating groups to the terminal ends of the dendrimer body with each additional layer called a “generation”. By varying the generations of synthesis, the amount of amine groups available for interaction can be controlled, with the most efficient dendrimer found to be the sixth generation in one study [33]. Significant delivery efficiency and improved biocompatibility has led

PAMAM to be widely used in *in vivo* studies [1]. These early polyplexes suffered from cytotoxicity as well as interactions and agglomeration with circulating serum proteins, leading to immunogenic side-effects.

While these initial vectors struggled with various extra- and intracellular barriers, their versatile chemistry allows for rapid production and alteration of specific lipids or polymers to deal with issues through subsequent generations. Where the virus has a protein capsid to retain genetic material, cationic polymers can be altered to increase charge density to better bind to DNA [1]. The viral mechanism of endosomal escape can be mimicked with membrane-disrupting moieties or polyethylenimine's proposed proton-sponge effect. While viruses evolved to target specific cell types or systems, lipids and polymers can be directly modified with various targeting moieties to increase uptake and overall efficiency in targeted cell populations. The various toxicity and immunogenicity issues of viruses can be alleviated with so-called "stealth coatings" like polyethylene glycol or various other polymers and polysaccharides [34]. It is only a matter of time before researchers adapt non-viral vectors to match the efficiency of viral vectors.

1.4 Characteristics of Anionic Polyplexes

To move beyond the first-generation binary polyplexes, research has moved to improving upon this platform by synthesizing specific polymers for new binary complexes or adding on additional materials to pre-existing binary complexes. Both of these strategies aim to improve upon initial binary particle interactions on overcoming various gene delivery barriers. The latter of these strategies involves the incorporation of additional layers upon the initial binary particle. This additional layer of material can include anionic polymer or monomer, neutral polymer, or cell-targeting polymers, among

others [35]. These ternary layers can provide immune avoidance characteristics, cell-specific targeting capabilities, or simply reduce toxicity inherent to many cationic delivery vectors. These characteristics can be incorporated by controlling particle surface chemistry and charge along with incorporating targeting moieties for specific disease states or cells. Here, ternary particles exhibiting an anionic surface charge will be discussed as one of these improvement avenues.

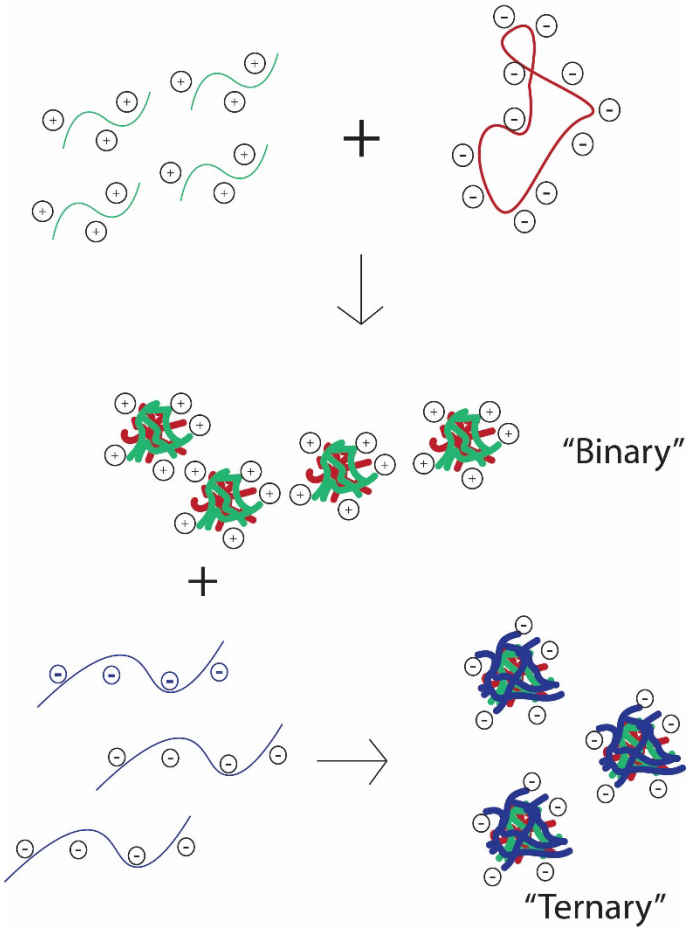

Figure 4 Ternary Polyplex Formation Schematic

1.4.1 Circulation Improvements

As briefly mentioned in an earlier section, initial binary polyplexes suffered in circulation from potential interactions and agglomeration with circulating serum proteins, leading to further phagocytic uptake or reticuloendothelial system clearance [36, 37]. These interactions will rapidly clear the delivery vector upon i.v. injection and cause the gene therapy treatment to be ineffective. Given that many of these circulating proteins and erythrocytes exhibit a negative surface charge, addition of an anionic ternary layer at a concentration to create a negative surface charge should mitigate these interactions. Kurosaki et al. [38] previously showed that the incorporation of various anionic polymers with cationic binary particles noticeably decreased agglomeration with mouse erythrocytes. Previous research in the Pack lab has indeed found that the addition of the anionic polymer, poly-L-glutamic acid, to binary particles comprising the reporter plasmid, pGL3, and the cationic polymer, polyethylenimine (PEI), led to a lesser degree of agglomeration with bovine serum albumin, as a model serum protein [39]. Studies utilizing a similar particle composition have found lowered cytotoxicity and agglomeration in murine models, illustrating this effect *in vivo* as well [40].

1.4.2 Lowered Cell Uptake

By the same mechanism that anionic ternary polyplexes can avoid agglomeration with negative serum proteins, the predominantly negative composition of the cell surface can also inhibit interaction with these polyplexes. In previous research, it has been shown that positive binary PEI polyplexes proceed down a caveolar uptake pathway, which has

proven beneficial for eventual transfection efficiency [41]. Multiple studies have noted decreased cellular uptake when adding various anionic polymers to similar PEI-based binary polyplexes [38, 39]. To investigate possible charge effects on uptake, Mott et al. formed ternary polyplexes from PEI-based binary complexes and the addition of an anionic polyglutamic acid layer. In comparing this combination with both positive and negative surface charges, this group found that anionic polyplexes proceed down a different endocytic pathway than their cationic counterparts [39]. Anionic particles were shown to be taken up predominantly through a clathrin-mediated endocytic pathway which is known to traffic to lysosomes and likely degrades the polyplexes. Lysosomal degradation is also proposed to significantly decrease transfection efficiency of these particles in addition to their already decreased cellular uptake.

1.4.3 Cytotoxicity Improvements

Multiple studies have reported the high cellular toxicity of cationic polyplexes, particularly PEI-based polyplexes [38, 39, 42]. Moghimi et al. proposed a two-step explanation for this cytotoxicity [42]. The first of these is caused by cell membrane disruptions caused by interactions with PEI, often leading to membrane pore formation. The second stage is a similar disruption in the membrane of the mitochondria, causing apoptosis to begin. These membrane disrupting effects have also been shown to be of potential benefit to gene delivery, however, as PEI has been proposed to stabilize holes and pores in the nuclear membrane to create stable pores for DNA entry [43]. Both Kurosaki et al. and Mott et al. found that the addition of a ternary layer led to decreased cytotoxicity in the cell lines investigated [38, 39]. The encapsulation of the toxic binary

particle through the use of the anionic polymer appears to alleviate some of the toxic effects of the PEI used in these studied systems.

1.5 Folic Acid-Related Therapeutics

Folic acid is a water-soluble vitamin (B9) necessary for DNA synthesis and repair. Folic acid is specifically used to synthesize thymine [44]. As cancer is a rapidly proliferating cell type, many cancers have evolved to overexpress folate receptor on their cell surface to increase uptake of this important molecule. Folate receptor comes in three isoforms, α, β, and γ, with the α isoform being the most prevalent and relevant to cancer therapeutics due to its higher binding affinity with folic acid [45]. The prevalence of folate receptor has even been investigated as a prognostic factor in human ovarian cancer and its increased concentration has been found to be positively correlated with poor chemotherapy response [46].

Given the significant overexpression of folate receptor in certain cancers, multiple therapeutics and diagnostic tools have utilized folic acid for targeting purposes. For example, Yoo et al. [47] conjugated the cancer drug doxorubicin to folic acid through a PEG linker. This study found that nanoaggregates of this targeted doxorubicin supported increased cellular uptake and decreased cell viability in tumor cells over-expressing folate receptor. Yin et al. [48] utilized folic acid's targeting ability to generate targeted carbon nanotubes as MRI contrast agents to better visualize human cervical cancer cells. It is also known that folic acid, while endocytosed through a receptor-mediated pathway, targets associated cargo through a caveolar endocytic pathway [41], which can be beneficial for certain therapies to avoid lysosomal degradation.

Folic acid has also been used as a backbone to generate standalone therapeutics. Methotrexate, a popular chemotherapeutic drug, was developed to be structurally analogous to folic acid for its increased uptake in cancer cells [44]. Methotrexate is thought to work as a chemotherapeutic through functioning as an antifolate and inhibiting the function of dihydrofolate reductase, which ultimately hinders a cell's ability to produce purines for DNA synthesis and repair [49]. Additional folic acid supplementation is encouraged in patients to alleviate harm to non-cancerous cells.

1.6 Concluding Remarks

The field of gene therapy is still an exciting field of research as numerous barriers to continued therapies are explored with alterations on various vectors. While viral vectors remain the peak of delivery efficiency, safety and ethical concerns plague its continued use in clinical settings. Multiple non-viral therapies are emerging rapidly to address the barriers facing both their use in gene delivery and their competition with viral therapies. Ternary polyplexes aim to address some of the circulation and toxicity issues with their binary counterparts, but are still shown to suffer in cellular uptake and transfection efficiency. Perhaps folic acid, a promising targeting agent used in both therapeutics and diagnostics, can be used to further improve existing gene delivery vehicles to better approach the efficiency of viral particles.

CHAPTER 2. DEVELOPMENT OF FOLATE-RECEPTOR TARGETED TERNARY POLYPLEX FOR GENE DELIVERY

2.1 Introduction

Polymeric gene delivery vectors remain a promising avenue of research as an alternative to currently available viral vectors. While polymeric vectors suffer in terms of transfection efficiency when compared to their viral counterparts, lower immunogenicity and facile modification make polyplexes potentially capable of repeated dosing and easy adaptation to suit various disease states. In particular, polyethylenimine (PEI) has shown early promise in binary polyplexes with high in vitro transfection efficiency and noted efficacy in multiple cell types [30]. These binary particles suffer, though, in terms of toxicity and serum agglomeration [1]. To remedy these issues, new generations of polyplexes have incorporated ternary polymeric layers for the purposes of immune shielding and reducing cytotoxicity [50]. Previous research in our lab [39] using poly(L-α-glutamic acid) (PGA) as a tertiary component has shown that the addition of this anionic polymer to the extent of making the polyplex negatively charged reduced cytotoxicity as well as decreased interactions with serum proteins.

These aforementioned anionic PGA/PEI/DNA ternary particles improved upon binary polyplexes' cytotoxicity, but suffered in terms of gene delivery efficiency. This study found decreased transfection efficiency and uptake in the negatively charged particles. While membrane repulsion between the negatively charged particles and the overall negatively charged cell surface partially explains the deficit in cellular uptake, the significant decrease in transfection efficiency was elucidated through an endocytic

pathway investigation. Mott et al. found that the negative particles were preferentially internalized via a clathrin-mediated pathway, leading to lysosomal trafficking and ultimate degradation of the particles.

In order to improve upon various delivery platforms, folate-receptor targeting has been proposed and utilized [44]. Attaching a folic acid ligand to the exterior of a delivery vector allows for interaction and uptake with folate receptor-α (FRα). Through this target, a delivery vector preferentially enters the cell through a lipid raft pathway typically associated with caveolin [44]. This pathway has been shown to avoid lysosomal degradation, allowing for improved delivery of genetic cargo. Folate-receptor targeting also preferentially targets cancer cells, as overexpression of FRα is established to confer a growth advantage for tumors as folic acid is utilized in DNA synthesis and repair [51]. This combination of targeting ability makes this an ideal scheme for the improved performance of gene delivery vectors.

To combine the reduced cytotoxicity and serum agglomeration found in anionic complexes with the preferential endocytic uptake of non-lysosomal pathways, the following study proposes the use of a folic acid receptor targeting schema to be added to an anionic polyplex to preferentially direct polyplexes down a caveolar endocytic pathway. To accomplish this, folic acid was conjugated in multiple ratios to PGA through a short polyethylene glycol linker and transfection efficiency of these particles was assessed.

2.2 Materials and Methods

2.2.1 Cell Culture

HeLa and HEK 293 cell lines with their associated cell culture media (EMEM and DMEM, respectively) were purchased from ATCC. Cell culture was performed according to ATCC protocol in appropriate cell media supplemented with 10% fetal bovine serum (FBS) at 37°C and 5% CO_2. Phosphate buffered saline (GE Life Sciences, 10 mM Na_2HPO_4, 1.8 mM KH_2PO_4, 137 mM NaCl, pH 7.2) was used to wash cells while trypsin (Corning, 0.53mM EDTA) was used to dissociate cells. Cells were lysed with a lysis reagent comprising 25 mM Tris-Phosphate buffer, 0.7 g/L 1,2-diaminocyclohexane, 10% glycerol, 1% Triton X-100, and 1% protease inhibitor cocktail (Millipore) at pH 7.8.

2.2.2 Materials

pGL3, a reporter plasmid encoding for firefly luciferase under control of the SV40 promoter-enhancer, was purchased from GenScript. Polyethylenimine (branched, 25 kDa) and CM Sephadex C-50 were purchased from Sigma-Aldrich. Poly-L-α-glutamic acid sodium salt (15 kDa) was purchased from Alamanda Polymers. Folate-linked PEG600 (FA-PEG-NH_2) was purchased from BioChemPEG. Dimethyl sulfoxide (DMSO) was purchased from Corning. Deuterium oxide was purchased from Acros Organics. Dimethyl sulphoxide-d6, 1-ethyl-3-(3-dimethylaminopropyl) carbodiimide (EDC), N-hydroxysuccinimide (NHS), and Slide-A-Lyzer dialysis cassettes (3,500 MWCO) were purchased from Thermo Scientific. Zetasizer folded capillary cells were purchased from Malvern.

2.2.3 Synthesis of Folic Acid-PGA Conjugate

Synthesis of folate-tagged PGA followed the scheme denoted in Figure 2. First, 10 mg/mL PGA was dissolved in a 2:1 DMSO:H_2O mixture and the carboxylate groups were activated with 10x molar excess EDC and 15x molar excess NHS, both in DMSO, for 15 min at room temperature with constant stirring. Chosen molar ratios of FA-PEG-NH_2 (1, 3, and 7x molar) based on the reported PGA MW of 15,000 kDa were then added and allowed to mix under constant stirring for 2 h at room temperature. Following the 2 h, 2 mL ß-mercaptoethanol was added to quench excess EDC before diluting the mixture 4x with water to allow for dialysis. Dialysis was performed using a 3,500 MWCO Slide-a-Lyzer dialysis cassette at room temperature against 3.5 L of MilliQ water with regular buffer renewal at 2, 4, and 12 h. Following dialysis, the product was run through a BioRad Econo-Column (1 x 20cm) loaded with CM Sephadex C-50 gel to remove any potentially remaining unreacted folic acid from the solution. Product was eluted with MilliQ water through gravity-driven flow and fractions collected through visual inspection of the yellow color attributed to the folic acid-associated polymer. Product was then lyophilized for 2 days, sealed, and stored in a -4˚C freezer for later characterization and use.

2.2.4 Verification of Folic Acid conjugation

A 0.5 mg sample of the PGA-Folate lyophilization products were dissolved in DMSO for folic acid quantification. 0.5 mg samples were dissolved in 0.5 mL DMSO and absorbance at 363 nm was read on a BioTek Synergy 2 plate reader in a clear quartz

bottom plate. This absorbance was compared to a standard curve of known folic acid concentrations to determine folate concentration on the polymer. This method found a folate ratio of 1.1, 3.2, and 7.1 for the three tagged polymers [referred to as PGA-Fol(1), PGA-Fol(3), and PGA-Fol(7), respectively].

2.2.5 NMR

NMR samples were prepared in DMSO-d6 or deuterium oxide as appropriate for solubility. Samples were added to Wilmad Economy NMR sample tubes and analyzed in a Bruker AVANCE NEO 600 MHz high-performance digital NMR spectrometer. Multiple 1D and 2D spectra were collected from the samples, including ^{1}H, ^{13}C, ^{15}N, COSY, HMBC, HSQC, and NOESY. The combination of these spectra was used to identify associated peaks and establish that the polymer modification had been completed properly.

Poly-L-α-glutamic acid **(1)**: ^{1}H NMR (90:10 H_2O:D_2O, 400 MHz): δ_H 1.84 (H4”), 1.93 (H4’), 2.18 (H5), 4.23 (H3), 8.49 (H2).

Folate-PEG600-NH_2 **(2)**: ^{1}H NMR (DMSO-d6, 600 MHz): δ_H 1.86 (H10), 2.14 (H11), 2.75 (H15), 3.19 (H14), 3.49 (H-PEG), 3.67 (H13), 4.29 (H9), 4.48 (H4), 6.65 (H6), 6.93 (H5), 7.03 (H2), 7.65 (H7), 7.88 (H2), 7.97 (H8), 8.14 (H12), 8.61 (H3). PGA-Fol(1) **(3)**: ^{1}H NMR (90:10 H_2O:D_2O, 600 MHz): δ_H 1.76 (H4, H8, H17), 1.89 (H9, H16), 2.27 (H5), 2.40 (H12, H14), 2.62 (H11), 3.32 (H13, H-PEG), 4.24 (H3, H7, H19), 4.48 (H24), 6.62 (H22), 6.98 (H23), 7.09 (H26), 7.16 (H21), 7.78 (H15), 8.04 (H2, H6), 8.15 (H10), 8.43 (H20), 8.64 (H25), 11.76 (br, H18).

PGA-Fol(3) **(4)**: ^{1}H NMR (90:10 H_2O:D_2O, 600 MHz): δ_H 1.93 (H4, H8, H17), 2.04 (H9, H16), 2.31 (H5), 2.48 (H12, H14), 2.68 (H27), 2.85 (H11), 3.66 (H13, H-PEG), 4.30 (H3, H7, H19), 4.42 (H24), 6.81 (H22), 7.39 (H23), 7.46 (H26), 7.64 (H21), 8.02 (H15), 8.41 (H2, H6), 8.51 (H10), 8.73 (H20), 9.13 (H25).

PGA-Fol(7) **(5)**: ^{1}H NMR (90:10 H_2O:D_2O, 600 MHz): δ_H 1.86 (H4, H8, H17), 1.98 (H9, H16), 2.21 (H5), 2.35 (H12, H14), 2.44 (H11), 3.61 (H13, H-PEG), 4.02 (H3, H7, H19), 4.22 (H24), 6.43 (H23), 6.75 (H22), 7.60 (H21), 7.99 (H15, H26), 8.39 (H2, H6), 8.45 (H10), 8.82 (H20), 9.05 (H25)

2.2.6 Gel Permeation Chromatography

Samples of PGA, PGA-Fol(1), PGA-Fol(3), and PGA-Fol(7) were prepared in HPLC grade water to a concentration of 5 mg/mL. Chromatography was carried out on an Agilent system with a 1260 Infinity II isocratic pump, degasser, and thermostated column chamber held at 30 °C containing Agilent PL Aquagel-OH column (300 mm). Water was used as the mobile phase at 1mL/min flow rate The system was equipped with a suite of detectors from Wyatt Technologies, which provided measurement of polymer concentration, molecular weight, and viscosity. Static light scattering was measured using a DAWN 8 Peltier system with differential refractive index measured with an Optilab.

2.2.7 Polyplex Formation

pGL3, PEI, PGA, and PGA-Fol stocks were generated by dilution in PBS to 0.1 mg/mL. Desired plasmid weight was then reached by diluting pGL3 stock in PBS to

accommodate 2 μg DNA per 20,000 cells. An appropriate volume of PEI stock was added to the diluted pGL3 stock in a 3:1 w:w ratio at room temperature to form binary polyplexes and allowed to incubate for 10 min. Ternary polyplexes were then formed by adding differing volumes of PGA or PGA-Fol under the same conditions for 10 min to achieve PGA/PEI/DNA ratio of 5.2:3:1 w:w:w.

2.2.8 Size and Zeta Potential

Particle size and zeta potential were measured using a Malvern Zetasizer Nano-ZS. Polyplexes were formed using the protocol described above at various PGA/PEI/pGL3 or PGA-Fol/PEI/pGL3 ratios containing 2 μg pGL3 and then diluted to 1 mL for size measurements or 0.75 mL for zeta potential measurements in 0.1X PBS. For size measurements, particles were transferred to a disposable cuvette and analyzed over 3 reads at 10 measurements per read. Zeta potential measurements were performed in Malvern Zetasizer folded capillary cells over 5 reads of 10 measurements each. All samples were run in triplicate and averaged.

2.2.9 Polyplex Transfection

HeLa and HEK 293 cells were transferred to a 96-well plate at 20,000 cells per well and allowed to attach for 24 h. Ternary polyplexes were then generated as described above. These polyplexes were then diluted to 100 μL with sterile media and supplemented with 5% FBS before being allowed to incubate for 5 minutes to allow for serum interaction. Ternary polyplexes were then incubated with the cells for 3 h in a 37

°C incubator. Following transfection, polyplexes were removed from the cells and the cells were allowed to incubate at 37 °C for 21 h in growth media. After this final incubation, cells were lysed with cell culture lysis reagent (CCLR), and the lysate was analyzed with Promega Luciferase Assay system in a BioTek Synergy 2 plate reader. Luciferase activities were normalized to total protein concentration in the lysates using a BCA assay.

2.3 Results and Discussion

2.3.1 PGA-Fol Synthesis and Conjugation Ratio Confirmation

Synthesis of the targeted polymer followed the scheme shown in Figure 5 and the method described above. PGA was weighed out to 15 mg as the starting material and dissolved to 10 mg/mL in a 2:1 v:v DMSO/water mixture. Carboxylate chains of PGA were activated with EDC/NHS and subsequently reacted with Fol-PEG600-NH_2. Amounts of EDC/NHS were chosen to modify 1, 3, or 7 side chains per polymer. Following the method described above, 8-12 mg of each PGA-Fol sample was collected after completed processing, indicating significant loss in product yield. All samples consistently appeared yellow in color with the intensity of color increasing with increasing folate conjugation ratio. To quantify the average number of folate moieties per polymer, the absorbance at 363 nm of each of the folate-conjugated PGA samples (1 mg/mL in DMSO) was compared to a standard curve of folic acid absorbance in DMSO at the same wavelength. These experiments determined that the folate ratios were 1.1, 3.2, and 7.1 for PGA-Fol(1), PGA-Fol(3), and PGA-Fol(7), respectively.

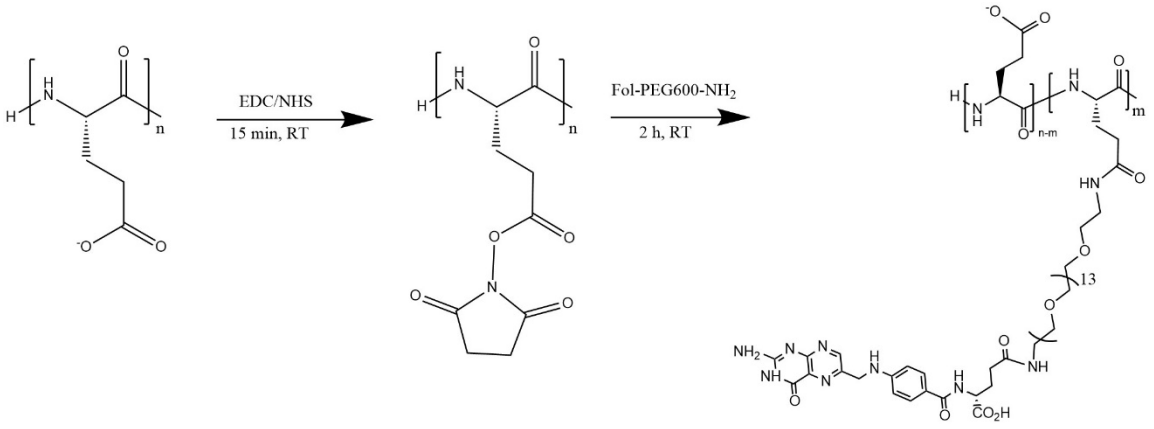

Figure 5 Chemistry scheme for the conjugation of folic acid to PGA through a PEG600 linker.

2.3.2 Chemical Structure Elucidation through Nuclear Magnetic Resonance

To better understand the final chemical structure of the conjugated polymer, various 1D and 2D NMR spectra were gathered on the conjugated polymers and starting materials. Using primarily a combination of ^{1}H, ^{13}C, HSQC, HMBC, and COSY spectra (see Appendix I), peak identification was performed on the spectra which aligns with the expected chemical structures of the finished products. The figures below illustrate the product of proton analysis (Figures 6-10). Peaks near 1 ppm appear in all samples and are adjacent to all peaks according to COSY spectra. These observations suggest that these peaks are not associated with the intended compound, but are instead contaminant peaks. Notably across all spectra, proper integrations could not be made to confirm the folate conjugation ratio. The only appropriate peak on the folate-free glutamic acid units to integrate against was the gamma carbon, which failed to provide a reasonable integration to any folic acid-associated peak. Recent work from Batys et al. suggests that this lack of

correlation might be due to the α-helix conformation of PGA in solution effectively hiding peaks from the NMR scans, leading to our noticeable lack of peak correlation [52].

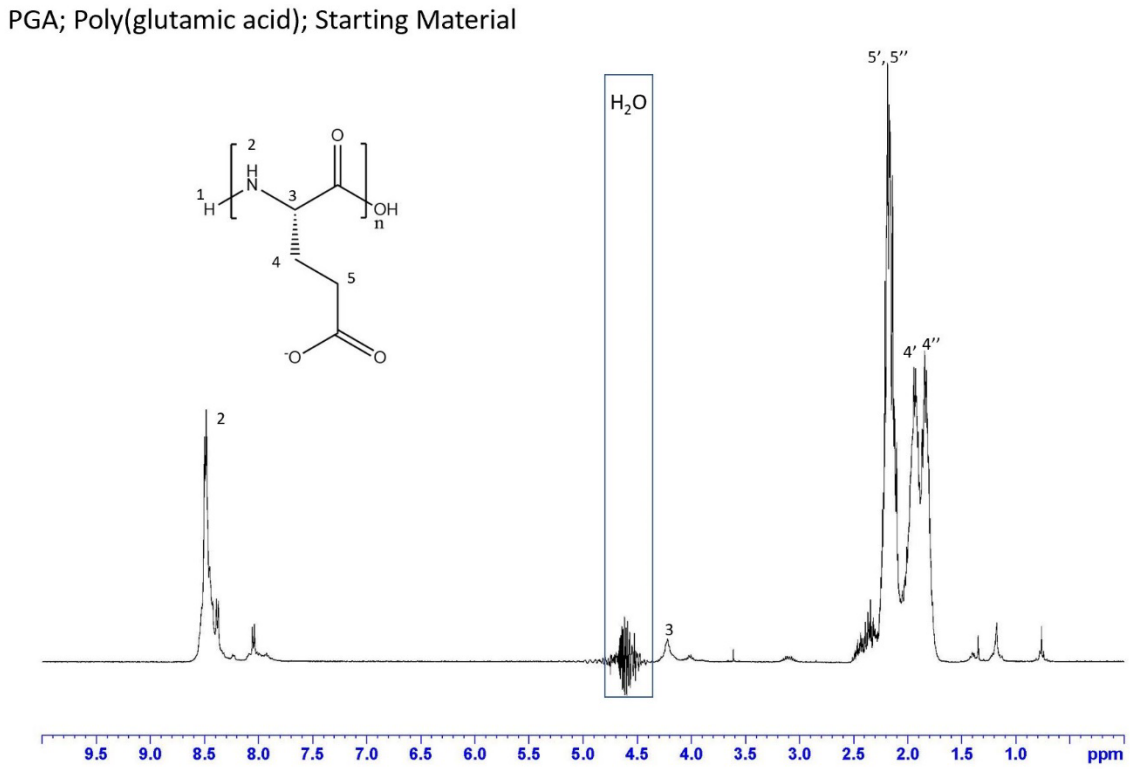

Figure 6 Proton NMR Spectra for the poly-L-α-glutamic acid starting material with peak identification

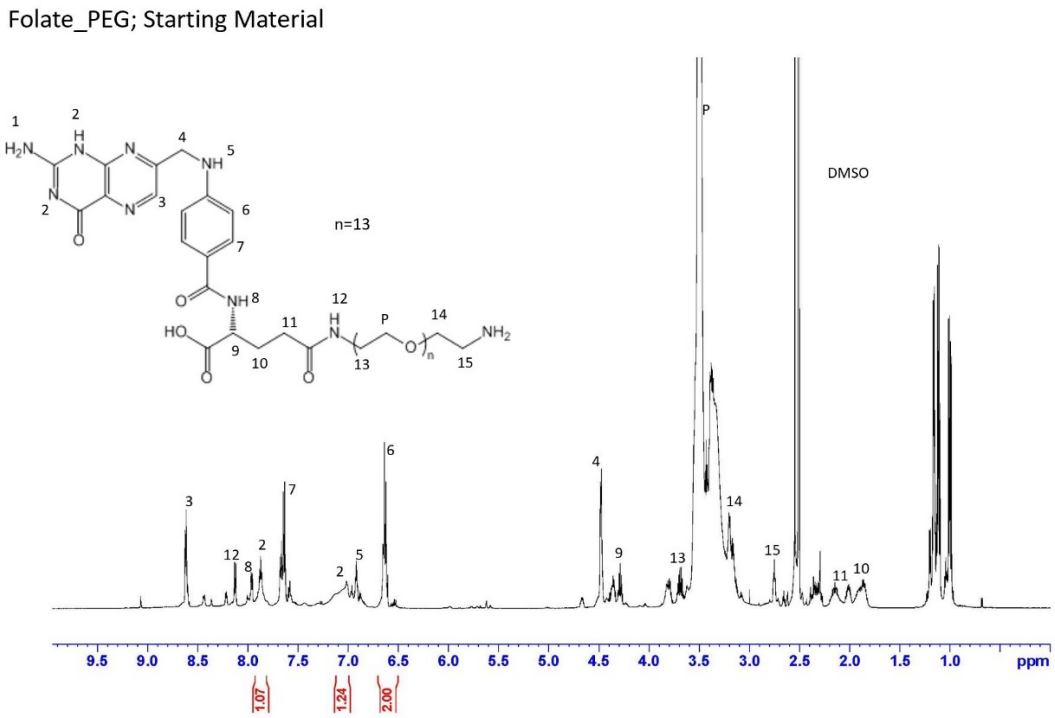

Figure 7 Proton NMR of Folate-PEG600-NH_2 starting material with peak identification

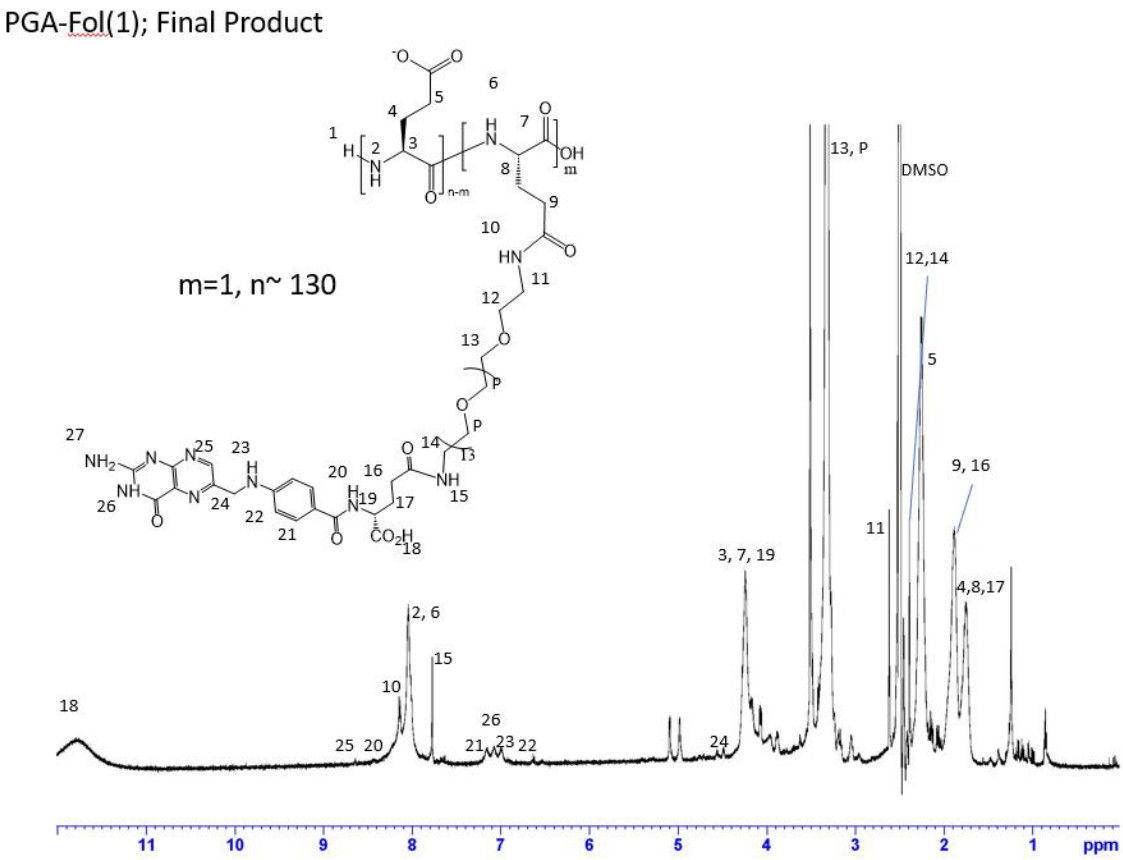

Figure 8 Proton NMR spectra and structure for PGA-Fol(1) with peak identification

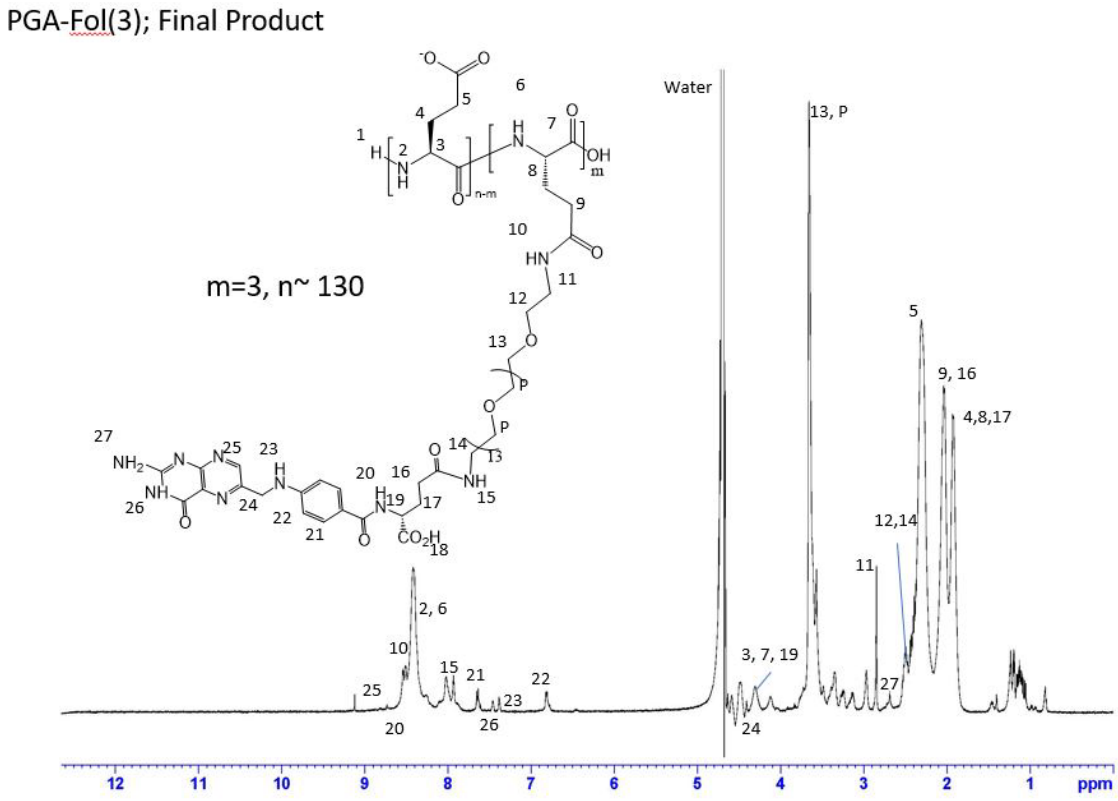

Figure 9 Proton NMR spectra and structure for PGA-Fol(3) with peak identification

PGA-Fol(7); Final Product

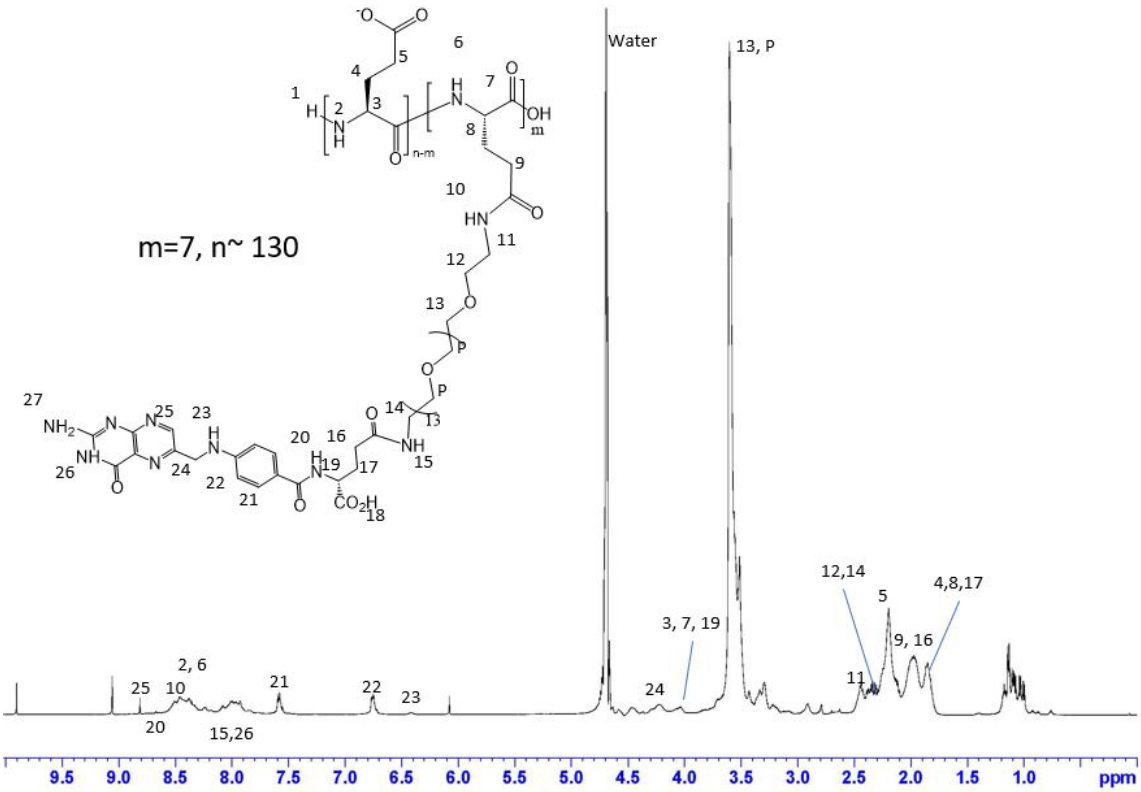

Figure 10 Proton NMR and structure for PGA-Fol(7) with peak identification

2.3.3 Crosslinking Determination through Gel Permeation Chromatography

In order to determine the potential inclusion of crosslinking or degradation in the targeted polymers, GPC was run on all samples. PGA as well as the three tagged polymers were dissolved in water and run through a size exclusion column before being read by a refractive index detector. Comparison between the PGA-Fol chromatographs and the starting material, PGA, was used to determine the potential for crosslinking or degradation of the completed polymer. Figure 11 illustrates that PGA-Fol(1) and PGA-Fol(3) are represented by clear, single peaks, indicating a lack of cross-linking or

potential degradation. These peaks also show little separation, consistent with the small difference in size that was expected. We expected that PGA-Fol(1) should be approximately 16 kDa and PGA-Fol(3) should be approximately 18.1 kDa. The PGA starting material and PGA-Fol(7) indicate the presence of two populations. The later peak of PGA-Fol(7) is likely unreacted PGA as it elutes at the same time as the PGA peak.

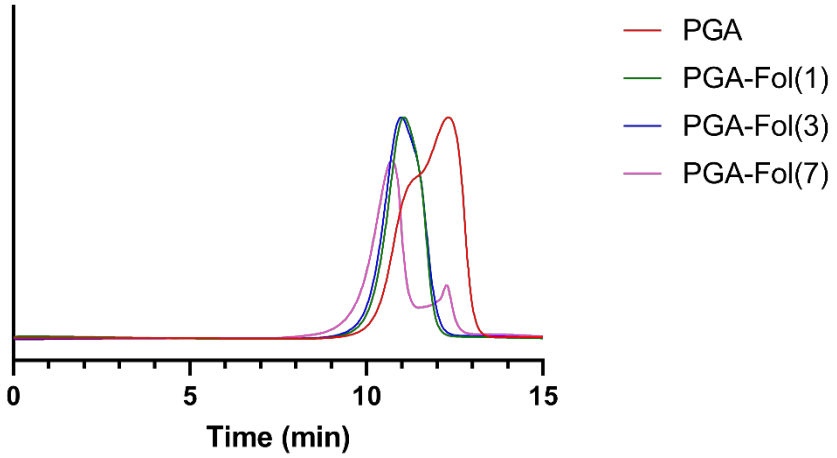

Figure 11 GPC chromatogram of PGA and PGA-Fol samples

2.3.4 Determining the Physicochemical Characteristics of Ternary PGA/PEI/DNA Polyplexes

PGA/PEI/DNA complexes were created at a w:w:w ratio of X:3:1. The 3:1 PEI/DNA ratio was chosen to remain comparable to previous data collected in the lab on non-folate conjugated polyplexes [39]. Hydrodynamic diameters of the ternary polyplexes exhibited a general trend of an approximately 200 nm increase in particle size upon addition of PGA to a 2:3:1 weight ratio (Figure 12). This is likely explained through the incorporation of additional material as well as the lessening of electrostatic forces

between the PEI and DNA with addition of PGA. These electrostatic forces serve to compact the binary particle components. Beyond the 2:3:1 w:w:w ratio, the size remained in the 400-500 nm range dependent on folate ratio. The asymptotic nature of the trend suggests that the size of the particle stabilizes as the electrostatic forces between the three components reach equilibrium with the addition of more PGA. The presence of folic acid does not appear to have a significant effect on the size of the particle, as expected with the addition of this relatively small targeting ligand.

Zeta potential measurements were performed to investigate the effect of folate conjugation on final polyplex charge. These data also serve to find the component ratio to generate anionic polyplexes. Zeta potential measurements on the various polyplex compositions displayed the expected downward trend in charge with the addition of the anionic polymer (Figure12). Conjugation of folic acid to the PGA sidechain, while replacing one negative charge group with another, also adds a positive amine group, leading to a slight increase in overall charge of the polymer. This can be seen with PGA-Fol(7) polyplexes remaining more positive than its lower folate ratio counterparts at the same 6:3:1 weight ratio. Using this information, subsequent particle transfections were performed at a 5.2:3:1 w:w:w ratio to ensure that all utilized particles fall in the negative surface charge range. This ratio also maintains consistency with existing anionic polyplex data collected previously by Mott et al. [39].

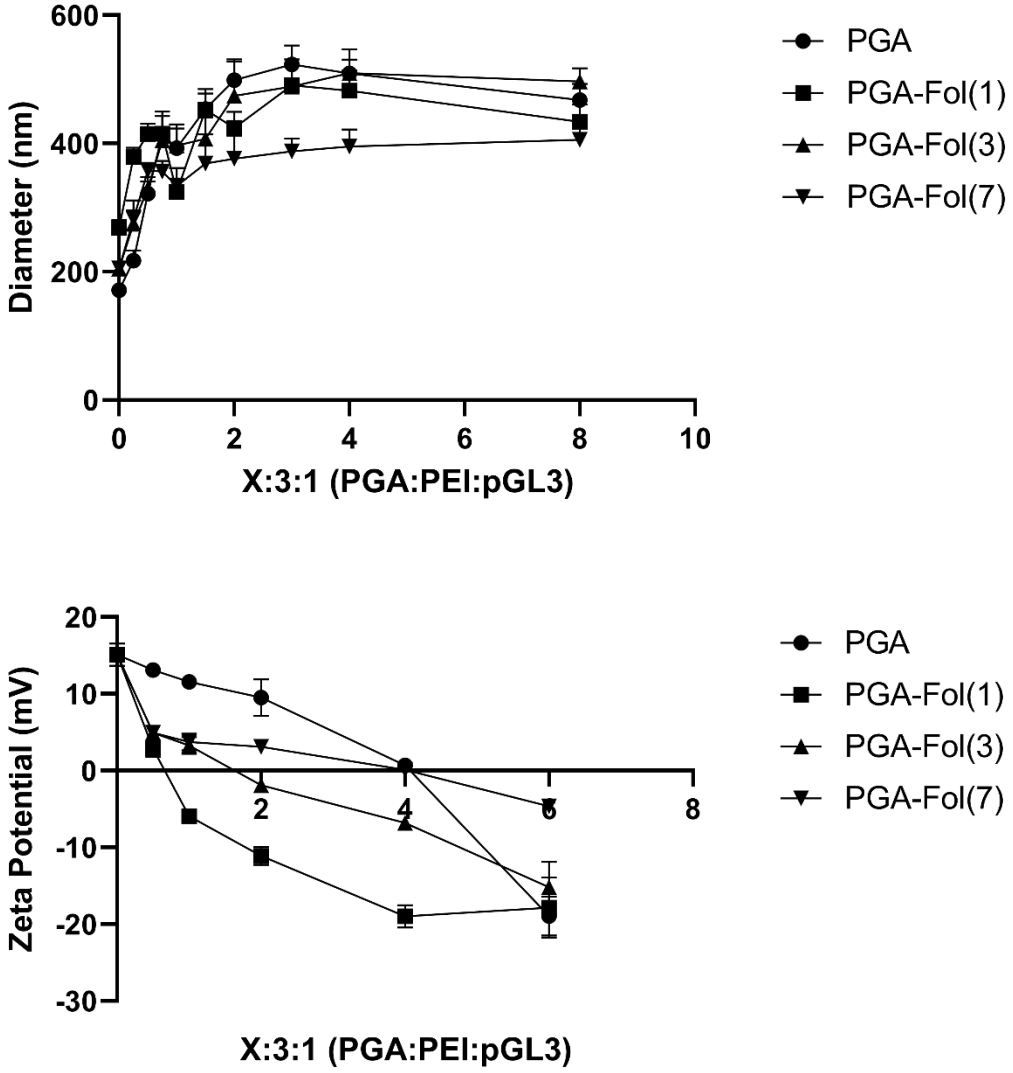

Figure 12 Dynamic Light Scattering and Zeta potential of a range of polyplex compositions and folate tag ratios. All polplexes formed at an X:3:1 PGA/PEI/DNA weight ratio.Error bars represent standard deviation

2.3.5 Folate-Receptor Targeting Viability as Determined by Transfection

Transfection studies serve as a simple investigation into the effect of the selected targeting scheme on ultimate genetic cargo delivery. As the particle must enter the cell,

traffic the cargo to the nucleus, and release the DNA, transfection studies confer results of the complete delivery process. In order to study the effect of folic acid receptor targeting, HeLa human cervical cancer cells were chosen as a folate receptor-positive cell line, while HEK 293 human embryonic kidney cells were chosen as folate receptor-negative line based on the relative receptor prevalence as reported by the Human Protein Atlas (1.4 nTPM for HEK 293 and 404.4 nTPM for HeLa; nTPM: normalized transcripts per million) [53]. Data shown in Figure 13 express the viability of this targeting scheme. Polyplexes were prepared at a 5.2:3:1 (PGA/PEI/DNA) weight ratio utilizing the range of generated PGA-Fol conjugates. These polyplexes were incubated with the chosen cell lines for 3 h in the presence of serum, and luciferase activity was assessed in cell lysates 24 h later. HeLa cells show a 1.6- to 2-fold increase in reporter expression in the PGA-Fol(1)/PEI/DNA and PGA-Fol(3)/PEI/DNA transfected cells compared to non-targeted polyplexes (Figure 13). Cells treated with PGA-Fol(7)/PEI/DNA polyplexes report lower luciferase expression than the untargeted polyplexes, consistent with previous studies in cationic polyplexes [41]. The high concentration of ligand on the particle surface can interfere with the intended pathway targeting and instead direct the particle down a non-specific uptake pathway, consistent with observations by Bandara et al. [54]. As expected of HEK 293 cells, the transfection data show an insignificant difference in luciferase signal following transfection with PGA-Fol(1)/PEI/DNA and PGA-Fol(3)/PEI/DNA polyplexes (Figure 13). Notably, the luciferase signal of HEK 293 cells transfected with PGA-Fol(7)/PEI/DNA polyplexes continues to be lower than all other treatments, again likely linked to a non-specific lysosomal uptake pathway.

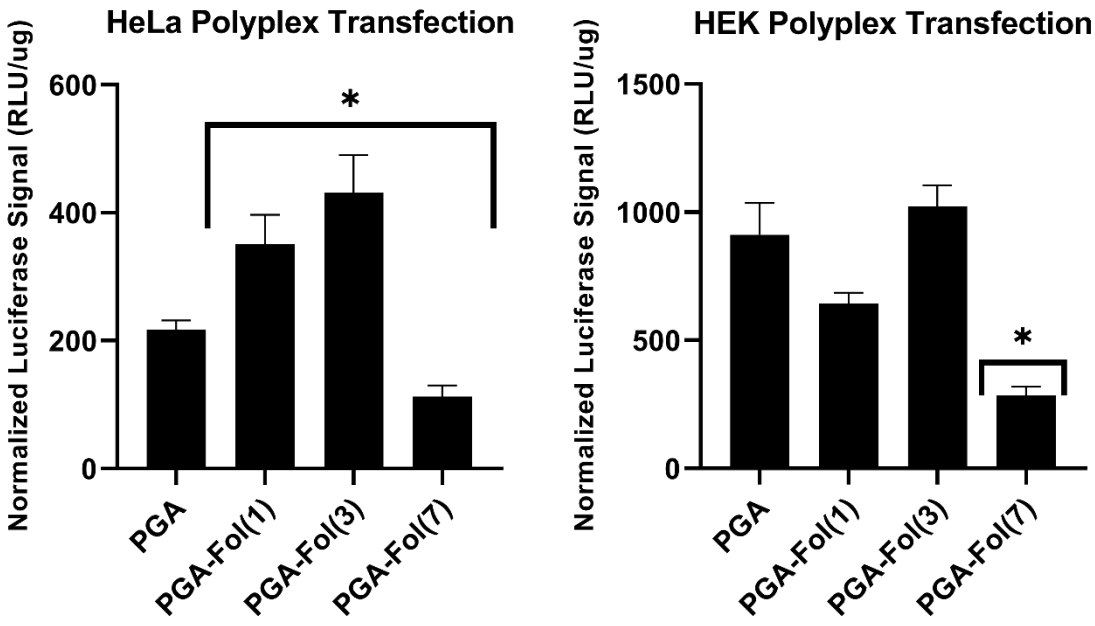

Figure 13 Targeted anionic polyplex transfection using various folic acid tagging ratios in both HeLa and HEK 293 cell lines. Particles were prepared at a 5.2:3:1 (PGA-Fol/PEI/DNA) weight ratio and incubated with cells in the presence of serum. (n=6, error bars represent standard error, *p<0.05)

2.4 Conclusions

Folic acid receptor targeting presents an exciting opportunity to improve upon the issues facing anionic ternary polyplex formations while still potentially maintaining the lowered cytotoxicity and serum agglomeration when compared to cationic formulations. The generation of folic acid conjugated PGA allows for the generation of such targeted anionic polyplexes for gene delivery. The various ratios of folate-tagged PGA were confirmed via various analytical techniques and further tested in folate receptor-positive and -negative cell lines. Transfection data showed an increase in transfection efficiency in HeLa cells using relatively low folate concentrations while higher concentrations led to a decrease in reporter expression. This is most likely due to the high density of targeting

ligand on the particle surface triggering a less-efficient, lysosomal pathway, as Bandara et al. noted in their study with multivalent liposomes [54]. In HEK 293 cells, we see little effect of folate targeting at low concentrations and a similar drop in transfection efficiency at the higher concentration, suggesting a sufficiently high level of conjugation of targeting ligand at which polyplexes might interact with the cell surface in such a way to trigger a non-specific uptake event. Further research is needed on these particles to elucidate their particular endocytic pathway of entry. Investigations into later nuclear transport pathways might also elucidate some of the discrepancy in transfection efficiency between the folate tag ratios seen here. This initial investigation gives promise to the folate receptor targeting scheme on this platform and further research will be done to elucidate the effects of folic acid conjugation.

CHAPTER 3. INVESTIGATION OF FOLATE RECEPTOR-TARGETING EFFECTS ON ENDOCYTIC UPTAKE PATHWAY

3.1 Introduction

Since the first successful gene therapy trial in 1990 [5], decades of research have sought to improve and expand upon current delivery methods. While viral vectors have seen multiple successes in gene delivery, these vectors suffer in terms of immunological side effects and possible random insertion [17]. Various synthetic delivery vectors have thus been developed to remedy these issues, but these new platforms now face efficiency issues that viruses have evolved to overcome. One possible method to improve upon these synthetic vectors is to investigate their endocytic path of entry and direct particles away from degradative or otherwise non-productive pathways.

The term "endocytosis" serves as an umbrella term for many processes a cell can use to take up nutrients or other substances [13]. The primary pathways under this umbrella, accounting for the majority of uptake, are clathrin-mediated endocytosis (CME), caveolin-mediated endocytosis (CvME), and macropinocytosis (MP) [8, 9, 13]. Clathrin-mediated endocytosis was formerly referred to as receptor-mediated endocytosis until this was proven to be misleading as most pathways can include receptor-mediated interactions [10]. CME is characterized by the generation of a clathrin shell that encapsulates the endocytic vesicle as it forms and is brought into the cell. This vesicle then acidifies to pH ~6 before progressing to late endosomes and fusing with lysosomes where the pH drops again to pH 5-6 [8, 10]. Acidification of the endolysosomal system along with the abundance of hydrolytic enzymes make CME and other lysosomal-

trafficking pathways hazardous to gene delivery vectors and should be avoided to allow for improved gene delivery.

Caveolin-associated endocytosis exists as a subdomain of lipid raft endocytic pathways [55]. Lipid rafts are membrane microdomains rich in cholesterol and sphingolipids. CvME is a further subdomain of lipid raft pathways in which the cholesterol-rich invagination is further enriched with caveolin-1. Vesicles resulting from CvME are thought to avoid lysosomal degradation, instead transporting cargo directly to the Golgi or endoplasmic reticulum [10]. As such, this pathway serves as a gentler route into the cell for any delivery vector.

Finally, macropinocytosis is a large-scale fluid uptake mechanism involving a cell membrane protrusion that collects surrounding fluid and associated solutes before fusing back into the cell membrane [13]. This process forms an endocytic vesicle termed a "macropinosome." This vesicle proceeds similarly to CME, first acidifying the vesicle and eventually fusing with lysosomes for cargo degradation. While the large-scale uptake mechanism of this pathway can be beneficial for the uptake of vectors, the subsequent degradative pathway serves to decrease the viability of this pathway for targeting or gene delivery.

Multiple physical and chemical characteristics of a delivery vector can affect the pathway of internalization. Rejman et al. demonstrated that particles have a preferential pathway determined simply by their size [12]. This study found that particles devoid of any targeting are endocytosed via a clathrin-mediated pathway when formed less than 200 nm, but then switched to a caveolin-mediated pathway at larger sizes, up until 1

micron. Mott et al., among others, have also demonstrated the effect of particle surface charge on internalization [39, 56, 57]. The ternary polyplexes used in Mott's study exhibited a preference toward caveolar endocytosis when the surface was cationic, but switched to predominantly clathrin-mediated endocytosis when anionic. Gabrielson et al. found similar results with cationic binary polyplexes, as well [41]. Perhaps the most obvious route to endocytic targeting is the use of targeting ligands. To target particles to a clathrin-mediated internalization pathway, researchers have incorporated ligands such as transferrin, low-density lipoprotein, or epidermal growth factor onto delivery vehicles [1, 58, 59]. Similarly, folic acid receptor and many GPI-anchored receptors internalize through the caveolar pathway [13, 41, 60].

The following study explored utilizing a combination of particle physical and chemical characteristics to direct particles to desired cell types as well as specific endocytic pathways. Building from the ternary polyplex platform of Mott [39], ternary anionic polyplexes were targeted to caveolin-mediated endocytosis through conjugation with folic acid to target folate receptor-α. Mott showed that these anionic polyplexes demonstrate decreased toxicity and serum agglomeration when compared to cationic particles, but suffered in terms of transfection efficiency and particle uptake. This study serves to demonstrate the effects of combining the beneficial qualities of anionic polyplexes with the targetability of folic acid.

3.2 Materials and Methods

3.2.1 Cell Culture

HeLa and HEK 293 cell lines with their associated cell culture media (EMEM and DMEM, respectively) were purchased from ATCC. Cell culture was performed according to ATCC protocol in appropriate cell media supplemented with 10% fetal bovine serum (FBS) at 37°C and 5% CO_2. Phosphate buffered saline (GE Life Sciences,10 mM Na_2HPO_4, 1.8 mM KH_2PO_4, 137 mM NaCl, pH 7.2) was used to wash cells while trypsin (Corning, 0.53mM EDTA) was used to dissociate cells. Cells were lysed with a lysis reagent comprising 25 mM Tris-Phosphate buffer, 0.7 g/L 1,2-diaminocyclohexane, 10% glycerol, 1% Triton X-100, and 1% protease inhibitor cocktail (Millipore) at pH 7.8.

3.2.2 Materials

pGL3, a reporter plasmid encoding for firefly luciferase under control of the SV40 promoter-enhancer, was purchased from GenScript. Polyethylenimine (branched, 25 kDa) was purchased from Sigma-Aldrich. Poly-L-α-glutamic acid sodium salt (15 kDa) was purchased from Alamanda Polymers. Genistein, methyl-ß-cyclodextrin, chlorpromazine, amantadine, and amiloride were purchased from Sigma Aldrich. Dharmafect was purchased from Fisher Scientific. siCAV1, siCLTC, siFOLR1, and negative control siRNA were purchased from Dharmacon.

3.2.3 Polyplex Formation

pGL3, PEI, PGA, and PGA-Fol stocks were generated by dilution in PBS to 0.1 mg/mL. Desired plasmid weight was then reached by diluting pGL3 stock in PBS to accommodate 2 mg DNA per 200,000 cells. An appropriate volume of PEI stock was added to the diluted pGL3 stock in a 3:1 w:w ratio at room temperature to form binary polyplexes and allowed to incubate for 10 min. Ternary polyplexes were then formed by adding differing volumes of PGA or PGA-Fol under the same conditions for 10 minutes to achieve PGA/PEI/DNA ratio of 5.2:3:1 w:w:w.

3.2.4 Transfection in the Presence of Endocytic Inhibitors

HeLa and HEK 293 cells were transferred to a 96-well plate at 20,000 cells per well and allowed to attach for 24 h. Small molecule endocytic inhibitors were prepared in DMSO or water as appropriate for dissolution. These concentrations were established in previous work to meet an 80% cell viability upon 4 h incubation with the cell types in question. Fifty microliters of each inhibitor solution were incubated with cells for one hour prior to addition of polyplexes. Ternary polyplexes were then generated as described above utilizing various tag ratios of folic acid. These polyplexes were then diluted to 100 μL with sterile media and supplemented with 5% FBS before being allowed to incubate for 5 min to allow for serum interaction. Ternary polyplexes were then incubated with the cells for 3 h in a 37 °C incubator. Following transfection, polyplexes were removed from the cells and the cells were allowed to incubate at 37 °C for 21 h in appropriate growth media. After this final incubation, cells were lysed with cell culture lysis reagent (CCLR)

and the lysate was analyzed with Promega Luciferase Assay system in a BioTek Synergy 2 plate reader. Luciferase values were normalized to well protein through a BCA assay.

3.2.5 Polyplex Uptake in the Presence of Endocytic Inhibitors

HeLa and HEK 293 cells were transferred to a 24-well plate at 200,000 cells per well and allowed to attach for 24 h. Small molecule endocytic inhibitors were prepared in DMSO or water as appropriate for dissolution as described in Table 1. Two hundred microliters of each inhibitor solution were incubated with cells for one hour prior to addition of polyplexes. pGL3 plasmid was fluorescently labeled with YOYO-1 iodide (Invitrogen) at 1 dye/50 bp, and polyplexes were prepared following the protocol described above. These polyplexes were then diluted to 500 µL with sterile media and supplemented with 5% FBS before being allowed to incubate for 5 min to allow for serum interaction. Ternary polyplexes were then incubated with the cells for 3 h in a 37 °C incubator. After 3 h, the polyplexes were removed, and the cells were washed once with PBS and dissociated with 200 µL trypsin. After approximately 10 min, the trypsin was neutralized by addition of 50 µL FBS, and 750 µL PBS was added to bring the total volume in each well to 1 mL. Collected cell samples were analyzed on an Attune Acoustic Focusing Cytometer (ThermoFisher). Cytometry data were analyzed with FlowJo data analysis software. Standard gating techniques were used to remove cell debris and calculate mean fluorescence.

3.2.6 siRNA Knockdown

HeLa and HEK 293 cells were transferred to a 6-well plate at 250,000 cells per cell and allowed to attach for 24 h. siRNA for caveolin-1 (CAV1), clathrin heavy chain (CLTC), folate receptor-α (FOLR1), and a non-targeted siRNA (siScramble) were mixed with Dharmafect transfection agent according to Dharmacon protocol. Cells were incubated with the resulting particles for 6 h in a 37 °C incubator. Following siRNA incubation, media was replaced with appropriate growth media and cells were allowed to incubate for 24 h. siRNA incubated cells were then counted and transferred to a 96-well plate at 20,000 cells per well and allowed to attach for 24 h. Transfection of these cells then proceeded according to the transfection protocol listed above in the absence of endocytic inhibitors.

3.3 Results and Discussion

3.3.1 Transfection Efficiency of Folate Receptor-Targeted Particles Relies on Caveolin and Lipid Raft-Dependent Pathways

HeLa and HEK 293 cells were chosen for this study as folate receptor-α positive and negative cell lines, respectively, due to their relative expression of FOLR1 as reported by the Human Protein Atlas [53]. HeLa cells contain 404.4 transcripts per million (TPM) while HEK 293 cells only have 1.4 TPM. Cells were first incubated with the various endocytic inhibitors described in Table 1 for 1 h before being transfected with anionic PGA/PEI/DNA polyplexes for 3 h. The resultant effects on transfection efficiency were measured via the reporter gene, firefly luciferase. For the purposes of

Figure 14, a decrease in luciferase signal indicates inhibition of a pathway beneficial to gene delivery. All particles show that uptake through caveolin and lipid raft endocytosis in HeLa cells is effective for gene delivery, as seen through the ~50-98% decrease in luciferase expression in both cell lines when exposed to genistein or MβCD. This trend in the folate-free particles is consistent with data acquired previously [39]. Decreases in expression under these conditions indicate that the polyplexes are taken up through an endocytic pathway which likely features lysosomal degradation, such as clathrin-mediated endocytosis or macropinocytosis. The reliance on these pathways is expected with folate-conjugated particles as this is the primary pathway for internalization of folate receptor. Further, decreases of ~50-70% in luciferase signal in the presence of the clathrin inhibitors suggest that the folate receptor-targeting is not enough to fully steer the particles away from their anionic preferences entirely. Finally, reliance on macropinocytosis as visualized through amiloride incubation is consistent with the pathways' large scale fluid uptake as well as its upregulation in cancer cell lines [14].

Table 1 Summary table of endocytic inhibitors

Inhibitor	**Pathway: Mechanism**	**Concentration; HeLa**	**Concentration; HEK 293**
Genistein	Caveolin: Inhibit tyrosine kinase necessary for caveolar vesicle trafficking	100 mg/L	70 mg/L
Methyl-β-Cyclodextrin (MβCD)	Caveolin: Sequesters plasma membrane cholesterol, inhibiting lipid raft formation	10 g/L	18 g/L
Chlorpromazine	Clathrin: Stabilizes intracellular clathrin, prevents recycling to plasma membrane	15 mg/L	18 mg/L
Amantadine	Clathrin: Stabilizes intracellular clathrin, prevents recycling to plasma membrane	750 mg/L	0.65 mg/L
Amiloride	Macropinocytosis: Blocks membrane Na^+/H^+ channels	500 mg/L	0.3 mg/L

With regard to our representative folate receptor-α negative cell line, HEK 293, a strong reliance on lipid-raft endocytosis is clear. While chosen as a folate receptor-negative cell line, HEK 293 is not completely absent of FOLR1, but rather expresses the gene almost 300-fold less than HeLa cells. As such, some effects of folate receptor targeting could still be noticed as in the presence of MβCD. Additionally, PGA-Fol(7)/PEI/DNA polyplexes show lowered expression in nearly all cases, consistent with

a multi-valent interaction with the cell surface and activation of a lysosomal endocytic pathway, as has been previously noted in literature [54]. While all of the polyplexes likely interact with folate receptor-α, interaction with multiple receptors at once likely triggers a non-lipid raft-associated uptake pathway.

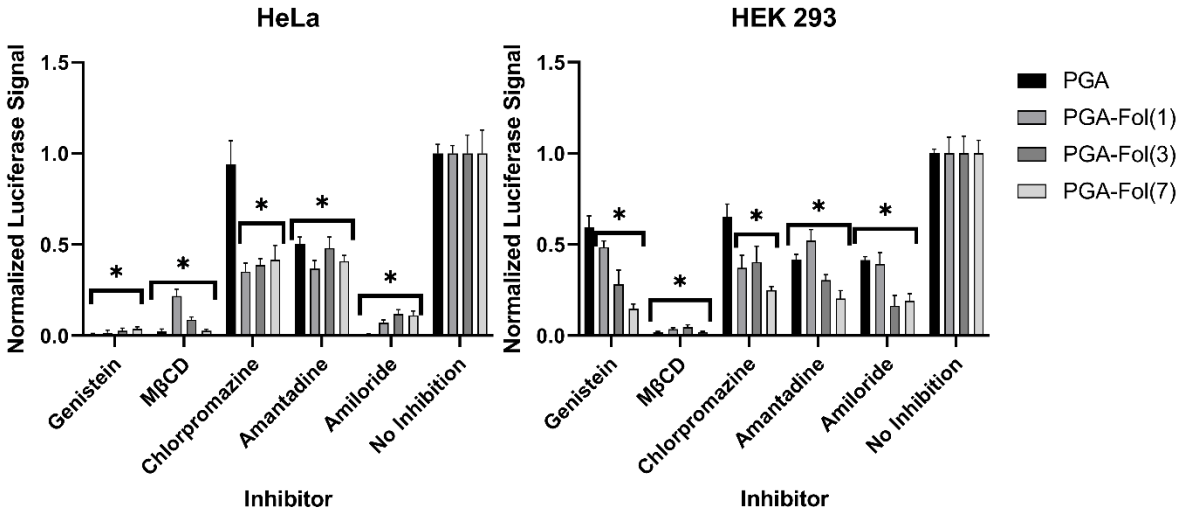

Figure 14 HeLa (left) and HEK 293 (right) cells were transfected with ternary polyplexes tagged with 1, 3, or 7 folates per PGA chain. Luciferase signal expresses gene delivery efficiency and all samples are normalized to non-inhibited controls (n=6, error bars represent standard error, *p<0.05 compared to non-inhibited cells)

In combination, the folate receptor targeting schema shows promise in these experiments with clear reliance on caveolin and lipid raft endocytosis pathways. Decreased luciferase expression with clathrin inhibitors in both cell lines was surprising as folate targeting should preference particles toward a caveolar-mediated pathway. Luciferase expression was expected to remain the same or potentially increase if clathrin-mediated pathways are inhibited. These data might suggest that the folate moiety is not sufficiently separated

from the particle, allowing for the presentation of negative charge effects in uptake. While this is not ideal in the realm of endocytosis, it does allow for the negative charge shell to continue resisting serum protein agglomeration without potential interference from the exterior folate tag.

3.3.2 Polyplex Uptake Effects of Folate Receptor Targeting

HeLa and HEK 293 cells were incubated with anionic ternary polyplexes and their uptake into the cell after 3 h in the presence of endocytic inhibitors was monitored via a YOYO-1 tag in flow cytometry. In Figure 15, a decrease in fluorescence should be interpreted as the inhibition of an effective uptake pathway. HeLa cells exhibit a noted decrease of ~50% in uptake of PGA-Fol(3)/PEI/DNA and PGA-Fol(7)/PEI/DNA polyplexes when inhibiting caveolar and lipid raft pathways, consistent with folate receptor-mediated uptake. The increase in uptake of non-targeted PGA polyplexes is likely indicative of upregulation of other endocytic pathways with the inhibition of caveolin. Minor decreases were noted in the uptake of PGA-Fol(1)/PEI/DNA and PGA/PEI/DNA polyplexes in the presence of chlorpromazine and amantadine, respectively. The decrease in uptake of the PGA/PEI/DNA polyplexes remained consistent with previously gathered data [39]. The combination of the effects of clathrin inhibitors here and in transfection experiments illustrates the lack of correlation between uptake and transfection. For example, while amantadine had little to no effect on particle uptake in HeLa cells, the resultant transfection of those particles was decreased ~50%. Inhibition of macropinocytosis through amiloride also causes a decrease in folate-targeted

polyplex uptake, consistent with interaction with membrane receptors and subsequent triggering of large-scale fluid uptake.

In the folate receptor-negative HEK 293 cell line, inhibition of clathrin-mediated uptake causes an increase in uptake of non-targeted particles, remaining consistent with previous data gathered by Mott [39]. Increases in uptake upon inhibition with MβCD reflect possible upregulation of non-lipid raft pathways. While the pathways explored in this study encompass the major pathways of endocytosis, many more pathways exist, and it remains possible that one of these unexplored pathways might be responsible for some of the increases in uptake upon inhibition of the expected caveolar or lipid-raft pathways.

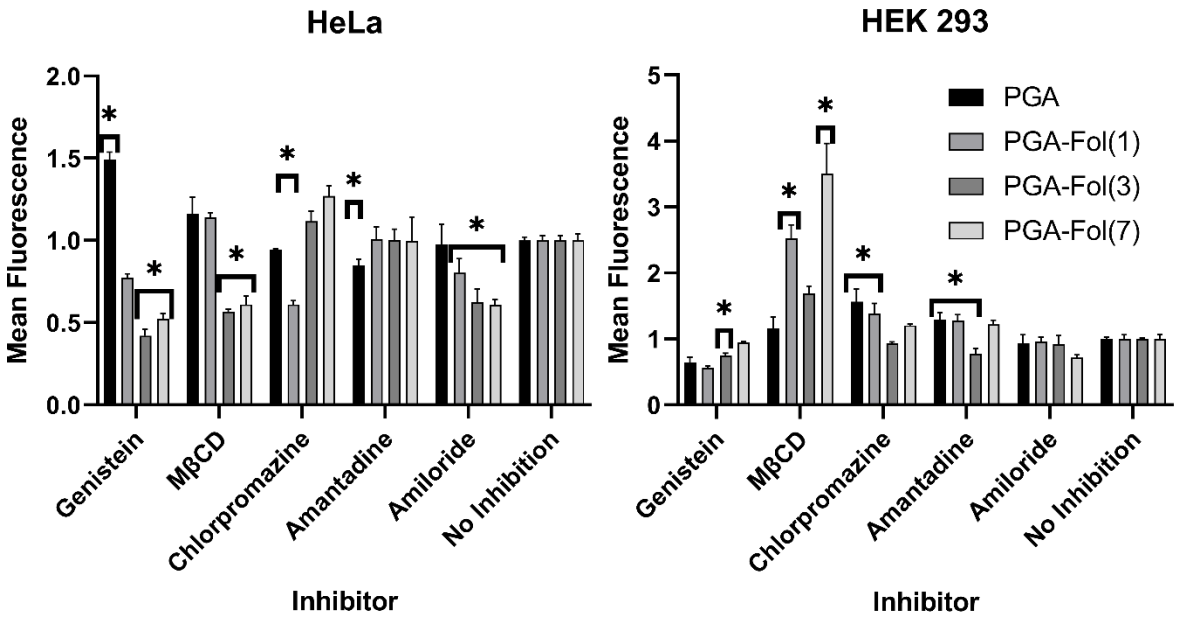

Figure 15 HeLa (left) and HEK 293 (right) transfected with YOYO-1 labeled polyplexes for flow cytometry measurement of particle uptake. All samples normalized to non-inhibited controls (n=3, error bars represent standard deviation, *p<0.05 compared to non-inhibited cells)

3.3.3 siRNA Knockdown Indicates Reliance on Lipid Raft Endocytic Pathway

Literature shows that many small molecule endocytic inhibitors are not specific to their intended pathway. This effect is often tied to the dose of the molecule used on the cells [61, 62]. As such, siRNA-mediated knockdown of the expression of key proteins required for specific endocytic pathways presents the opportunity to corroborate the effects of endocytic inhibitors. Thus, HeLa and HEK 293 cells were transfected with siRNA to knock down expression of endocytic proteins or folate receptor-α. In both HeLa and HEK 293 cells, CAV1 knockdown led to a significant increase (~1.5- to 3-fold) in transfection with all polyplex populations, with the exception of PGA-Fol(7)

particles. The cells lack the expected decrease in transfection efficiency upon knockdown of CAV1, indicating a lack of reliance on this pathway. Folate-conjugated particles exhibit the expected decrease in luciferase expression in HeLa cells, but do not show a complete elimination of signal. This illustrates that, while targeted to the folate receptor, the particles could still be internalized and lead to transfection, likely through charge-dependent pathways. CAV1 knockdown in combination with the decreased luciferase signal from FOLR1 knockdown suggests that the folate receptor-targeted particles are interacting with the intended receptor and are relying more heavily on lipid raft pathways independent of caveolin. This remains consistent with the small molecule inhibition results presented above. HeLa cells with CLTC knocked down exhibited a minor decrease in PGA-Fol(7)/PEI/DNA polyplex transfection, but show no effect on the other polyplex combinations. Generalized decrease in luciferase expression of the PGA-Fol(7) polyplexes in HeLa implies that while the particles are interacting with the intended receptor, they are triggering both caveolar uptake, as intended, and a lysosomal uptake pathway through multi-valent interactions with multiple receptors at once. In HEK 293, knockdown of CLTC increases luciferase signal in folate-conjugated particles by approximately 2-fold. Increased luciferase signal with the knockdown of CLTC suggests that the particles are traveling through a non-clathrin associated endocytic pathway and likely avoiding lysosomal degradation, leading to increased transfection. Similarly, luciferase signal is increased up to 3-fold in HEK 293 cells with folate-conjugated polyplexes. Increased luciferase signal upon inhibition of CAV1 indicates a possible lipid raft-based pathway, similar to the HeLa samples. We note no significant effect of FOLR1

knockdown in HEK 293 cells. This was expected from the low FOLR1 expression in this cell line.

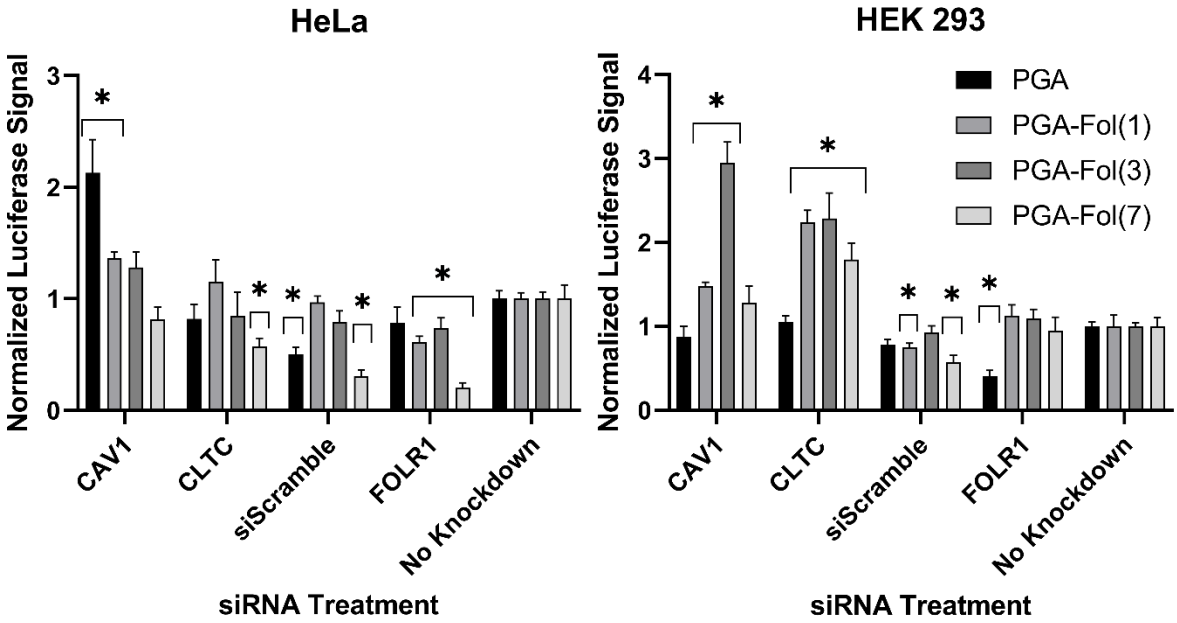

Figure 16 HeLa (left) and HEK 293 (right) cells were transfected with anionic polyplexes after specified endocytic pathways were knockdown via siRNA. (n=6, error bars represent standard error, *p<0.05 compared to cells which weren't knocked down)

3.4 Conclusions

Polymer-based gene delivery vectors face many continuing barriers to matching the capabilities of viral vectors. This study sought to overcome the barriers of targetability and endocytic entry. Using the folate receptor, anionic ternary polyplexes were targeted away from the degradative clathrin-mediated endocytic pathway that plagued anionic polyplexes in previous studies. Figure 17 illustrates the observed diversion away from clathrin-mediated uptake and toward a caveolin-associated pathway. Increased uptake through a caveolin- or lipid raft-associated pathway also encouraged more effective

transfection through avoidance of the lysosomal degradation pathway. Investigation through both small molecule endocytic inhibitors and siRNA knockdown of relevant proteins indicates that PGA-Fol(1) and PGA-Fol(3) particles successfully targeted folate receptor-α and enter the cell through a lipid raft-dependent endocytic pathway that can be caveolin-dependent or independent. PGA-Fol(7) likewise exhibits interaction with the appropriate receptor, but appears to enter through a number of endocytic pathways, likely due to a multivalent interaction with receptors. This result remains consistent with previous studies indicating that multivalent interaction with cell surface receptors can trigger non-specific uptake of the tagged cargo [54].

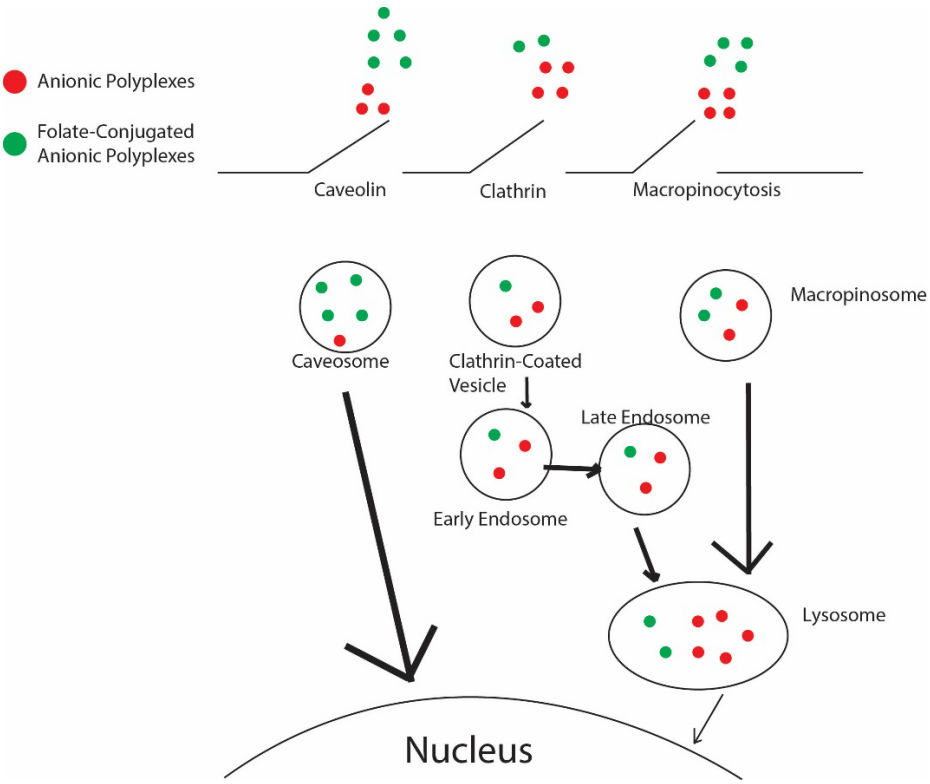

Figure 17 Pathway Summary for Targeted and non-Targeted Polyplexes

In order to better clarify the effects of folate receptor-targeting on endocytic entry, one might investigate particle uptake through microscopy using known markers of various endocytic pathways. For example, using transferrin or CLTC tag to track clathrin endosomes, CTxB or caveolin-1 tag for caveolar endosomes, and 70-kDa dextran to track macropinocytosis. Understanding that there are other possible pathways to entry, a large-scale siRNA screen of a wide array of endocytic-related proteins would elucidate more specific proteins and pathways related to polyplex entry. Additionally, data need to be collected to verify that these tagged polyplexes maintain their agglomeration avoidance in the presence of representative serum proteins. There is still much to be done to best understand the pathways anionic polyplexes travel to ultimately deliver their genetic

cargo and, further, the adaptations necessary to continue improving on the platform as a whole.

CHAPTER 4. INVESTIGATION OF FOLATE RECEPTOR-TARGETING EFFECTS ON INTRACELLULAR TRAFFICKING

4.1 Introduction

Gene delivery vectors face many barriers to transport their genetic cargo to the nucleus. Upon administration, the particle must traverse the circulatory system while avoiding serum agglomeration and immune system activation before reaching the cells of interest. Vectors must then interact with the cell, internalize, and transport their cargo to or near the nucleus. There exist two major pathways to accomplish this last step. The first is passive Brownian diffusion through the cytoplasm. While this is a viable option for some vectors, large (>30nm [63]) and charged particles will have difficulty navigating the densely packed cytoplasm, which lacks free movement space for delivery vectors. The alternative for large particles is then active transport within endocytic vesicles. Polymer-based gene delivery vectors have been heavily implicated to follow this method of translocation. Active transport is largely dependent on microtubules and small molecular motors called dynein and kinesin. These molecular motors carry endocytic vesicles, along with entrapped cargo, by "walking" along microtubules. Distinction between the two motors is made via their direction of travel, with dynein traveling toward the "+" end of microtubules, or toward the nucleus, and kinesin traveling toward the "-" end, or away from the nucleus.

An array of small molecule inhibitors have been utilized to investigate the intracellular pathway of delivery vectors [64]. Microtubule involvement in particle transport can be probed through the use of colchicine and paclitaxel. Colchicine acts as a potent depolymerizer of microtubules, leaving dynein and kinesin without a track to move along [65]. Paclitaxel works counter to colchicine by stabilizing microtubules, but

limiting cellular motility through inhibiting tubulin recycling [65, 66]. Cytochalasin D is used to depolymerize actin filaments, which are implicated in both endocytic vesicle formation as well as early endosome trafficking [67]. ATPase inhibitors are utilized to inhibit the function of the molecular motors. Dynein, in particular, is inhibited with sodium orthovanadate and EHNA (erythro-9-[3-(2-hydroxynonyl)] adenine) [68, 69]. Kinesin, likewise, is inhibited by Rose Bengal lactone (RBL) and adenylylimidodiphosphate (AMP-PNP) [70, 71].

These aforementioned inhibitors have been used previously to investigate the intracellular trafficking of both cationic lipoplexes and polyplexes [64, 72]. In both cases, microtubule involvement was found to be strongly correlated to gene delivery, implying an active delivery scheme for these cationic vectors. Drake et al. further noted that molecular motors and actin played a significant role in the active transport of PEI/DNA binary complexes. Suh et al. utilized real-time particle tracking to visualize the transport of PEI/DNA polyplexes and similarly found that these complexes follow an active transport route [73]. Neither method has been utilized to investigate ternary anionic complexes.

Ternary anionic polyplexes have been developed to remedy issues plaguing cationic complexes, including increased cytotoxicity and serum protein agglomeration. While cationic complexes perform well *in vivo* in terms of transfection efficiency, their inherent toxicity and potential immune system activation limit their use in a clinical setting [39]. By utilizing anionic polymers in the formation of gene delivery polyplexes, the surface charge and other characteristics of the particle can be controlled. Early investigation into such polyplexes found that while they may avoid serum agglomeration

and exhibit decreased cytotoxicity, their overall transfection efficiency and uptake suffer [38, 39]. As such, folate-receptor targeted anionic polyplexes were developed as described in previous chapters. To better understand both the impact of surface charge and folate-receptor targeting on intracellular trafficking, the following study utilizes an array of small molecule inhibitors to probe the transport system used by such complexes.

4.2 Materials and Methods

4.2.1 Cell Culture

HeLa and HEK 293 cell lines with their associated cell culture media (EMEM and DMEM, respectively) were purchased from ATCC. Cell culture was performed according to ATCC protocol in appropriate cell media supplemented with 10% fetal bovine serum (FBS) at 37°C and 5% CO_2. Phosphate buffered saline (GE Life Sciences,10 mM Na_2HPO_4, 1.8 mM KH_2PO_4, 137 mM NaCl, pH 7.2) was used to wash cells while trypsin (Corning, 0.53mM EDTA) was used to dissociate cells. Cells were lysed with a lysis reagent comprising 25 mM Tris-Phosphate buffer, 0.7 g/L 1,2-diaminocyclohexane, 10% glycerol, 1% Triton X-100, and 1% protease inhibitor cocktail (Millipore) at pH 7.8.

4.2.2 Materials

pGL3, a reporter plasmid encoding for firefly luciferase under control of the SV40 promoter-enhancer, was purchased from GenScript. Polyethylenimine (branched, 25 kDa) was purchased from Sigma-Aldrich. Poly-L-α-glutamic acid sodium salt (15 kDa) was purchased from Alamanda Polymers. Colchicine, paclitaxel, cytochalasin D,

EHNA HCl, sodium orthovanadate, and rose Bengal lactone were purchased from Sigma Aldrich. AMP-PNP was purchased from Roche.

4.2.3 Polyplex formation

pGL3, PEI, PGA, and PGA-Fol stocks were generated by dilution in PBS to 0.1 mg/mL. Desired plasmid weight was then reached by diluting pGL3 stock in PBS to an accommodate 2 μg DNA per 200,000 cells. An appropriate volume of PEI stock was added to the diluted pGL3 stock in a 3:1 w:w ratio at room temperature to form binary polyplexes and allowed to incubate for 10 min. Ternary polyplexes were then formed by adding differing volumes of PGA or PGA-Fol under the same conditions for 10 min to achieve PGA/PEI/DNA ratio of 5.2:3:1 w:w:w.

4.2.4 Intracellular Inhibitor Toxicity

Small molecule inhibitors of various points on the active intracellular transport path were chosen for this study. Their targets and mechanisms are described in Table 2. Each inhibitor was dissolved in DMSO or water as appropriate for solubility and mixed with appropriate sterile media for HeLa and HEK 293 cell lines. These stock concentrations were serially diluted to generate a concentration curve of each inhibitor for cell toxicity studies. The concentrations listed in Table 2 were the point at which 80% of the exposed cells remained metabolically viable after 4-h incubation at 37°C as demonstrated through a CellTiter-Blue assay (Promega). All concentrations are consistent with literature values for viable inhibitory concentrations [64]. These concentrations were used throughout the remaining polyplex transfection and uptake studies to follow.

Table 2 Summary table of intracellular inhibitors

Inhibitor	**Target**	**Concentration; HeLa**	**Concentration; HEK 293**
Colchicine	Binds to the end of microtubules to prevent elongation	2 μM	5 μM
Paclitaxel	Stabilizes microtubules	1 μM	1.5 μM
Cytochalasin D	Inhibits actin polymerization	5 μM	20 μM
EHNA Hydrochloride [Erythro-9-(2-hydroxy-3-nonyl)adenine]	Selective dynein inhibitor	1.25 mM	0.5 mM
Sodium Orthovanadate	Dynein inhibitor	200 μM	180 μM
AMP-PNP [adenylyl-imidodiphosphate]	Competitive inhibitor of kinesin	3 mM	10 mM
Rose Bengal Lactone	Kinesin Inhibitor	70 μM	30 μM

4.2.5 Transfection in the Presence of Intracellular Trafficking Inhibitors

HeLa and HEK 293 cells were transferred to a 96-well plate at 20,000 cells per well and allowed to attach for 24 h. Small molecule intracellular trafficking inhibitors were prepared in DMSO or water as appropriate for dissolution, then diluted with appropriate sterile media to desired concentrations described in Table 2. Fifty microliters of each inhibitor solution were incubated with cells for one hour prior to addition of polyplexes. Ternary polyplexes were then generated as described above utilizing various

tag ratios of folic acid. These polyplexes were then diluted to 100 μL with sterile media and supplemented with 5% FBS before being allowed to incubate for 5 min to allow for serum interaction. Ternary polyplexes were then incubated with the cells for 3 h in a 37 °C incubator. Following transfection, polyplexes were removed from the cells and the cells were allowed to incubate at 37 °C for 21 h in appropriate growth media. After this final incubation, cells were lysed with cell culture lysis reagent (CCLR) and the lysate was analyzed with Promega Luciferase Assay system in a BioTek Synergy 2 plate reader. Luciferase values were normalized to well protein through a BCA assay.

4.2.6 Polyplex Uptake in the Presence of Intracellular Trafficking Inhibitors

HeLa and HEK 293 cells were transferred to a 24-well plate at 200,000 cells per well and allowed to attach for 24 h. Small molecule intracellular trafficking inhibitors were prepared in DMSO or water as appropriate for dissolution, then diluted with appropriate sterile media to desired concentrations described in Table 2. 200 μL of each inhibitor solution was incubated with cells for one hour prior to addition of polyplexes. pGL3 plasmid was fluorescently labeled with YOYO-1 iodide (Invitrogen) at 1 dye/50 bp, and polyplexes were prepared following the protocol described above. These polyplexes were then diluted to 500 μL with sterile media and supplemented with 5% FBS before being allowed to incubate for 5 min to allow for serum interaction. Ternary polyplexes were then incubated with the cells for 3 h in a 37 °C incubator. After 3 h, the polyplexes were removed, and the cells were washed once with PBS and dissociated with 200 μL trypsin. After approximately 10 min, the trypsin was neutralized by addition of 50 μL FBS, and 750 μL PBS was added to bring the total volume in each well to 1 mL.

Collected cell samples were analyzed on an Attune Acoustic Focusing Cytometer (ThermoFisher). Cytometry data were analyzed with FlowJo data analysis software. Standard gating techniques were used to remove cell debris and calculate mean fluorescence.

4.3 Results and Discussion

4.3.1 Intracellular Inhibitor Toxicity

Prior to intracellular pathway investigation, various intracellular inhibitors were tested for toxicity in HeLa and HEK 293 cells for a 4 h incubation period. Inhibitors were prepared as stock solutions in water or DMSO as appropriate for solubility and diluted in sterile cell media for each cell line for incubation. Inhibitor concentration which maintained 80% cell viability was chosen for later polyplex transfection and uptake studies. The summary of the toxicity data can be found in Table 2. These concentrations remain consistent with literature values for inhibition while maintaining cell viability. Colchicine caused significant toxicity in both cell lines at low concentrations. This was also true of paclitaxel and cytochalasin D in HEK 293 cells. This likely indicates the impact of microtubules and actin on the overall viability of the cell given their role in cell division.

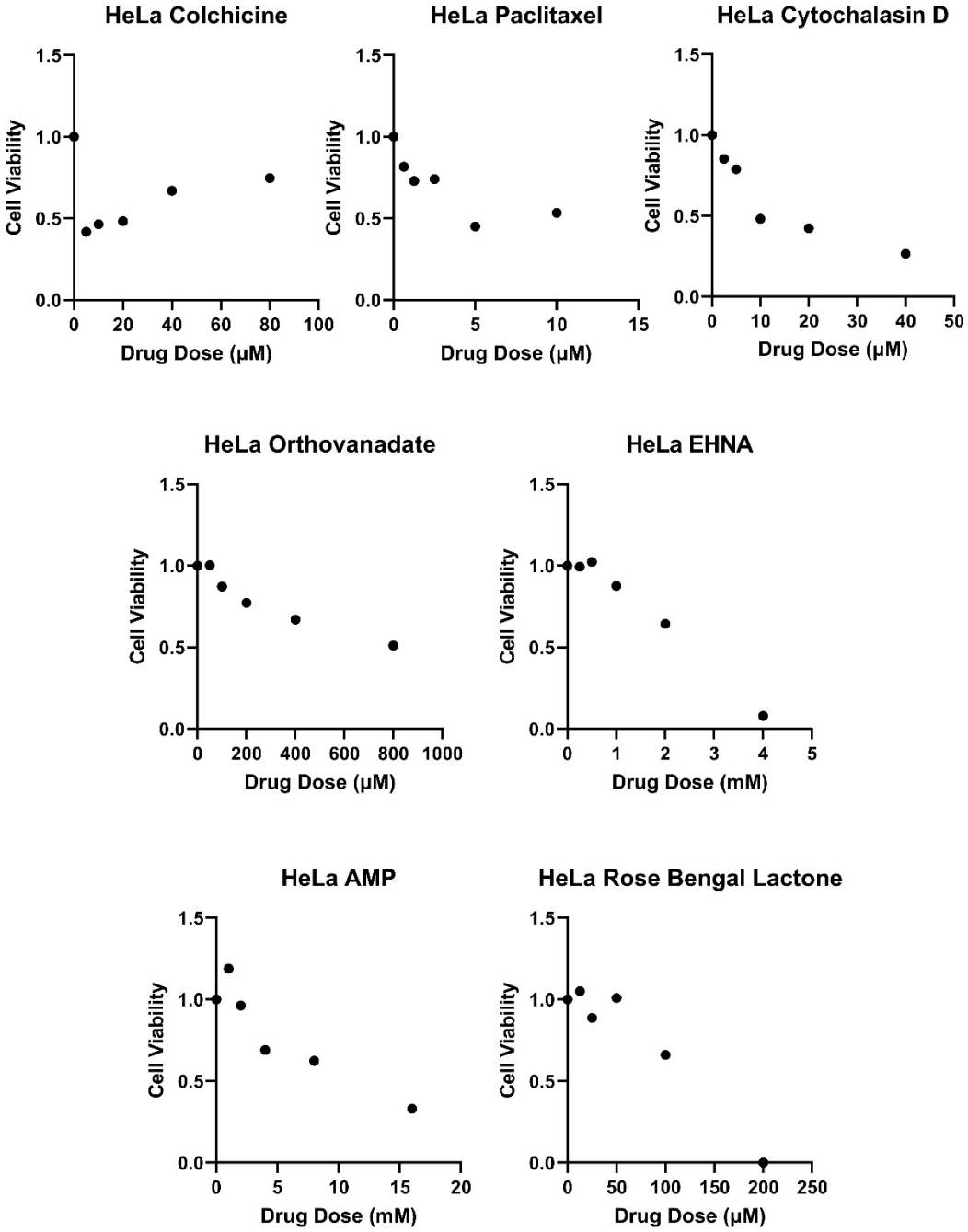

Figure 18 Intracellular Inhibitor Toxicity in HeLa cells. Concentration at 80% cell viability was taken for further polyplex experiments. (n=4)

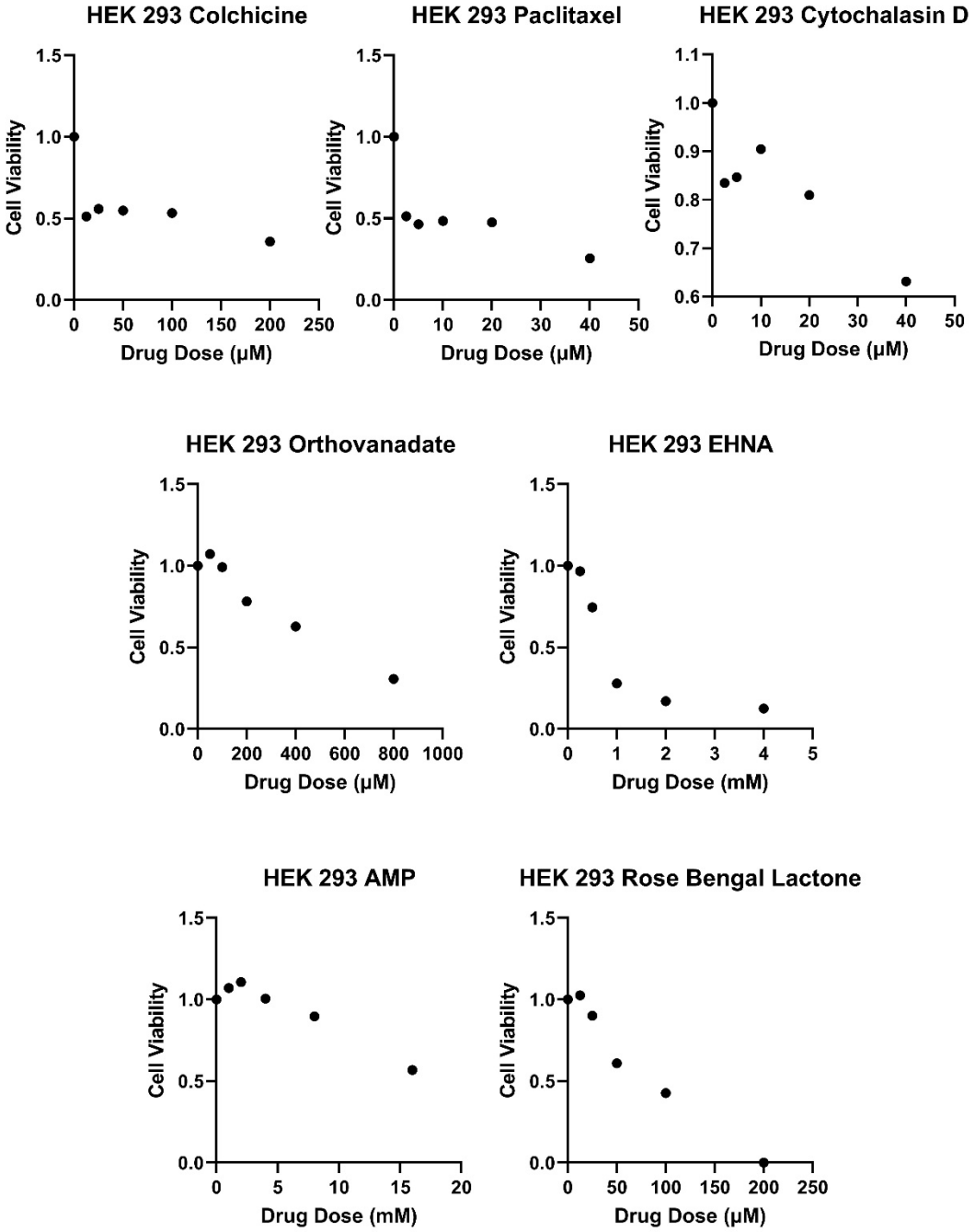

Figure 19 Intracellular Inhibitor Toxicity in HEK 293 cells. Concentration at 80% cell viability taken for further polyplex experiments. (n=4)

4.3.2 Reliance on Active Pathways for Transfection

HeLa and HEK 293 cells were transfected with folate-conjugated or folate-free ternary anionic polyplexes in the presence of small molecule inhibitors for various constituents of intracellular trafficking. In both HeLa and HEK 293 cells, colchicine incubation significantly decreased luciferase signal upon transfection with nearly all polyplex formulations by up to 90%. Similarly, paclitaxel incubation decreased luciferase signal in HeLa cells, with the exception of PGA-Fol(1)/PEI/DNA polyplexes. These data illustrate that microtubule involvement in transport is significant, with the exception of PGA-Fol(1)/PEI/DNA particles in HeLa. This was an unexpected result as it seems unlikely that PGA-Fol(1)/PEI/DNA polyplexes should be transported significantly differently from the other folate-conjugated particles. It remains possible that PGA-Fol(1)/PEI/DNA polyplexes continue down an active pathway as exhibited by decreased luciferase expression in the presence of orthovanadate and rose Bengal lactone, but this pathway may be microtubule independent. Inhibition of actin through cytochalasin D exposure decreased luciferase expression up to 97% across both cell lines, with all polyplex formulations exhibiting decreased luciferase expression by at least 50%. These data illustrate a strong reliance on actin for polyplex transfection. As actin is involved in both intracellular trafficking and various endocytic pathways, it remains unclear as to which step along the path actin is important to transfection with these vectors. This remains an area for future study. The molecular motors, dynein and kinesin, appear strongly tied to the transfection process of these polyplexes as the luciferase signal of cells treated with any of the folate-tagged polyplexes decreased when exposed to at least one of the various ATPase inhibitors. With the exception of PGA-Fol(1)/PEI/DNA

polyplexes, it appears the presence or absence of folate conjugation makes no difference in the progression of the polyplexes further into the cell. Additionally, both folate receptor positive and negative cell lines behaved similarly with respect to active transport.

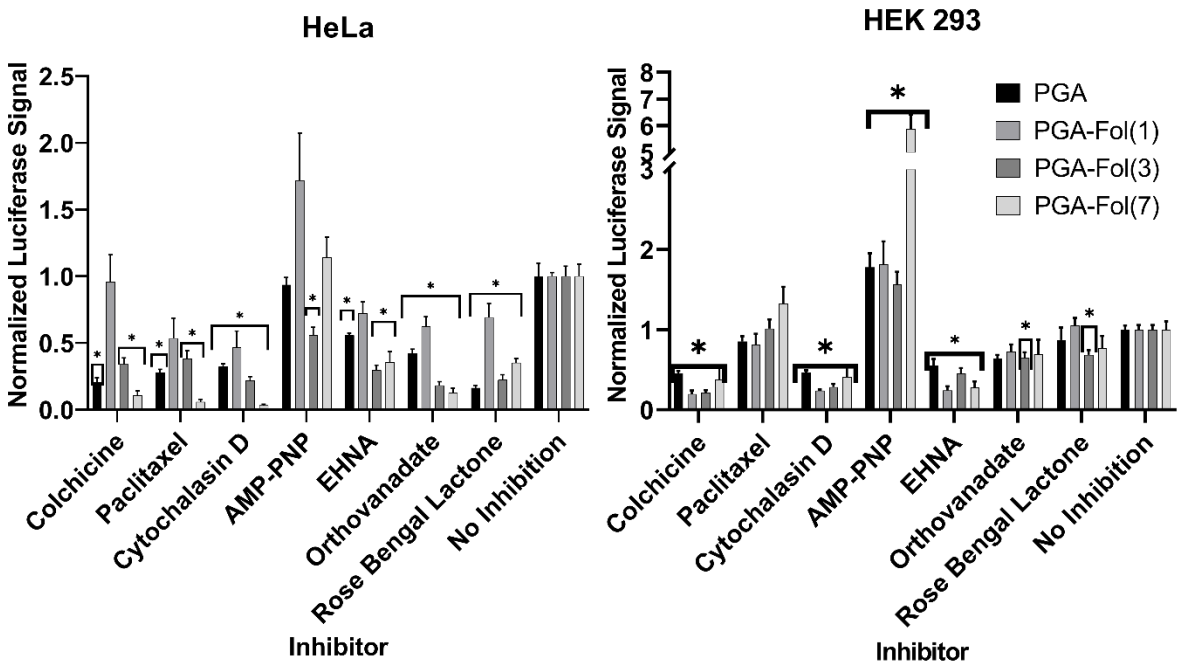

Figure 20 HeLa (left) and HEK 293 (right) were transfected with ternary anionic polyplexes in the presence and absence of various small molecule intracellular trafficking inhibitors. Luciferase expression is used as a measure of gene delivery efficiency. (n=6, error bars represent standard error, *p<0.05 compared to non-inhibited cells)

4.3.3 Polyplex Uptake Investigation through Flow Cytometry

HeLa and HEK 293 cells were incubated with ternary anionic polyplexes of various folate-conjugation ratios in the presence and absence of small molecule intracellular trafficking inhibitors. Colchicine and paclitaxel show differing results in this

experiment with paclitaxel showing no effect on particle uptake and colchicine inhibiting particle uptake in most cases by 40-50%. With the exception of PGA-Fol(1)/PEI/DNA polyplexes, these gene delivery vectors show reliance on microtubules for particle uptake as well as the previously mentioned transfection. As microtubules play a key role in cell division, it is possible that disrupting the natural cell cycle caused a decrease in particle uptake. As mentioned previously, actin is tied to both endocytic entry as well as early endosomal trafficking. As such, both cell lines exhibit some reliance on this pathway for particle uptake. PGA-Fol(1) again stands out as it exhibits an increase in uptake in HEK 293 cells when exposed to cytochalasin D, possibly implying a diversion away from actin-driven uptake is beneficial to eventual polyplex uptake. Further investigation into non-actin-dependent pathways in both endocytic and intracellular realms is necessary to better understand this result. While all ATPase inhibitor concentrations were chosen to maintain 80% viability, it remains possible that the concentrations of these inhibitors led to non-specific interactions with other ATPases aside from the intended molecular motors. The concentrations chosen were also consistent with inhibitory concentrations found by Drake et al. [64]. Significant decrease in uptake with multiple ATPase inhibitors, particularly AMP-PNP, indicates a possible non-specific inhibition of other ATP-driven pumps or motors. Further investigation into the role of molecular motors as related to polyplex active transport might involve more specific knockdown of such proteins with the use of siRNA interference. siRNA technology could also be utilized to investigate other actin-independent uptake pathways as noted with PGA-Fol(1).

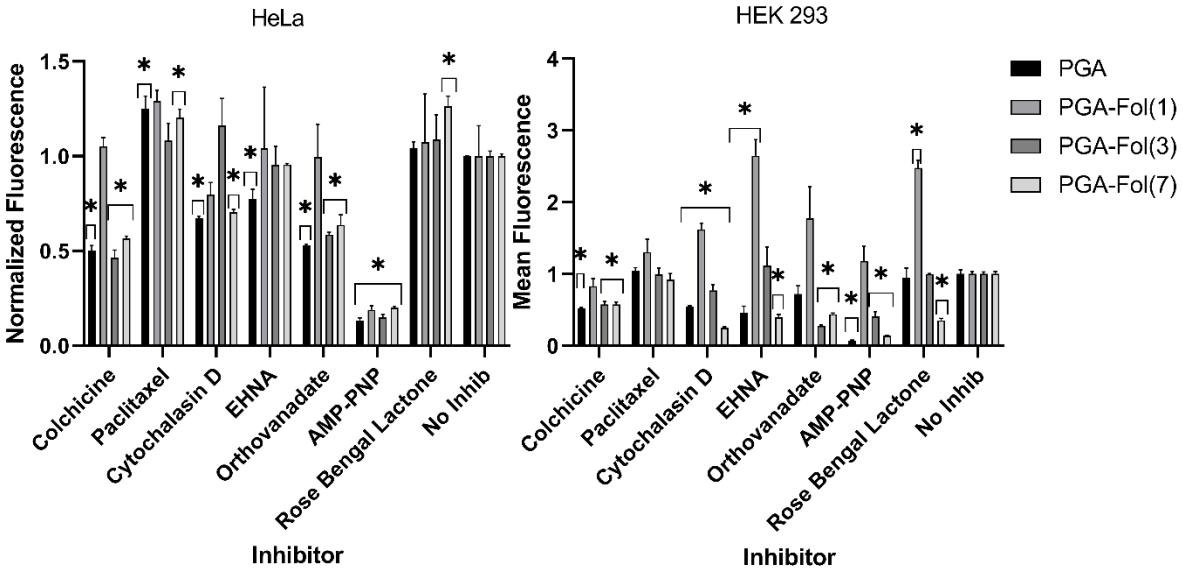

Figure 21 HeLa (left) and HEK 293 (right) were transfected with ternary anionic polyplexes tagged with a YOYO-1 DNA label in the presence and absence of various small molecule intracellular trafficking inhibitors. Mean fluorescence is used as a measure of particle uptake (n=3, error bars represent standard deviation, *p<0.05 compared to non-inhibited cells)

4.4 Conclusions

Polymer-based gene delivery vectors face many barriers before ultimately delivering their genetic cargo to the nucleus. One such barrier, intracellular trafficking, was investigated here with its impact on anionic ternary complexes. In summary, we have found that these gene delivery complexes rely significantly on actin filament and microtubule-dependent active transport for ultimate gene transfection. Generally, little to no difference was noted between folate-tagged and folate-free polyplexes in this regard. Actin involvement in this process could be attributed to its role in endocytosis or intracellular transport. For more specific investigation into the influence of these structures or the related molecular motors, an intensive siRNA knockdown screen for

these related proteins would be necessary to avoid non-specific effects of small molecule inhibitors. Regardless of these qualifications, active transport is still relevant to the intracellular trafficking of the studied complexes just as with previously studied cationic binary complexes [64, 73]. Reliance on active transport is likely tied to size and surface charge, whether positive or negative. This makes sense as a larger particle would have a more difficult time randomly traversing the organelle-packed cytoplasm as opposed to directed, active transport through the cell to the perinuclear region. As such, reliance on active transport is clear, though further investigation into the specifics of this transport are necessary.

CHAPTER 5. PERSPECTIVES AND FUTURE DIRECTIONS

The work presented throughout this dissertation was built on years of work before it and leads to further work for years beyond. The earliest instances of gene delivery relied on viral vectors which, while quite proficient at gene delivery, suffer in terms of repeat dosing and immunological interactions. In one of many attempts to remedy the issues of viral vectors, polymer-based delivery vectors were designed and developed. Early binary polyplexes formed of simple electrostatic interactions between cationic polymer and anionic DNA performed well in terms of plasmid transfection, but continued to suffer in regards to cytotoxicity and serum protein agglomeration. Again, one of many solutions to these issues was the development of ternary complexes which could better control the surface charge of the complete complex. Through this platform, surface charge was discovered to influence the endocytic pathway of entry for these particles. More specifically, cationic ternary complexes, similar to their binary counterparts, enter the cell through a caveolar pathway, thus avoiding the lysosomal degradation inherent to clathrin-dependent pathways. Anionic complexes suffered in terms of transfection efficiency as it was discovered that they are endocytosed through a clathrin-mediated pathway. However, these anionic complexes succeeded in decreasing cytotoxicity and serum agglomeration *in vivo*. Thus, the work of this dissertation focused on improving upon these anionic complexes through the use of cell and endocytic pathway targeting with the incorporation of folic acid.

Through the course of several studies, we found that these folate receptor-targeted ternary polyplexes divert some of the particle population away from the clathrin-

dependent pathway that their anionic nature directs them to and instead preferences the particles toward a lipid raft endocytic pathway, which is either caveolin-dependent or -independent. Further, utilizing a range of folate-tagging ratios, we confirmed previous literature findings that multivalent tagging of delivery vectors with folic acid leads to non-specific endocytic uptake. With our endocytic pathway of entry confirmed, we continued along the path to transfection and investigated the intracellular route of transport of our polyplexes to the perinuclear region of the cell. Generally speaking, both targeted and non-targeted polyplexes demonstrated clear reliance on active transport along microtubules through the use of molecular motors. This remains consistent with previous studies on cationic binary particles [64], implying that active transport reliance is tied to particle size and presence of charge.

Looking forward from the studies presented here, two paths seem evident: improving upon this collected knowledge and expanding beyond this dissertation. To first improve upon these findings, live-cell microscopy studies could be utilized in a few different ways. Colocalization studies with markers of specific endocytic compartments would demonstrate which pathways these targeted and non-targeted particles tend to follow. Such studies could also demonstrate potential differences in uptake rate between the particle populations. Similarly, live-cell particle tracking can be utilized to visualize the direct or random path of a delivery vector inside the cell. This technology could also be used in concert with FRET imaging to visualize where the polymer delivery vector dissociates from the genetic cargo, which is still a lively debate among researchers in the field. Departing from microscopy studies, the use of siRNA knockdown technology would greatly benefit the interpretation of the data presented here. As small molecule

inhibitors are known to be somewhat non-specific, especially at higher concentrations, specific inhibition of targeted proteins and enzymes would give a more specific and complete picture of the pathways utilized by these delivery platforms. For example, in the case of PGA-Fol(1) transport, we found that uptake of these particles specifically was not actin-dependent, as many of the major endocytic pathways are. Investigation of other endocytic and intracellular pathways through siRNA knockdown would present a better picture of the unique path that PGA-Fol(1)/PEI/DNA polyplexes utilize. Investigation of the impact of linker-length in relation to this platform might also be a useful route of continued study. As seen in the endocytic pathway investigation of chapter 3, folate-tagged particles did travel down caveolar pathways, but still showed significant reliance on clathrin-dependent endocytosis as well, likely owing to their anionic surface charge. As such, increasing the length of the linker to further separate folate from the charge effects of the particle has the potential to divert a greater percentage of the particle population away from a clathrin-mediated, degradative pathway.

In the interest of exploring beyond the ternary polyplexes studied here, a few different strategies could be explored or combined with these particles to further improve the field of gene delivery. While polyethylenimine remains strong in its ability to transfect cells due to a variety of chemical characteristics, its continued incorporation in delivery vectors is problematic due to its increased potential for membrane disruption and general cytotoxicity. Unfortunately for this polymer, the same characteristics that make it great for gene delivery also harm its potential use in a clinical setting. The adoption or development of biocompatible polymers for gene delivery will be ideal for the continued use of this platform and progress into the clinic. Development of such polymers should

also include some capability for controlled release of the genetic payload as the mechanism(s) of release of nucleic acid payloads in PEI-based complexes remains debated. I do believe that polymer-based therapies still show great promise overall in the field of gene delivery with their rapid and facile alteration potential and a great capacity to mimic the beneficial mechanisms of viral vectors.

APPENDIX

Methods:

NMR samples were prepared in DMSO-d6 or deuterium oxide as appropriate for solubility. Samples were added to Wilmad Economy NMR sample tubes and analyzed in a Bruker AVANCE NEO 600 MHz high-performance digital NMR spectrometer. All following appendix figures contain additional NMR spectra utilized to determine the ^{1}H NMR peaks for the samples shown in chapter 2. In the following instances, ^{13}C and ^{15}N HSQC were used to attribute protons to their associated carbons and nitrogens, respectively. COSY, TOCSY and NOESY, only shown for the Fol-PEG sample, were used to determine relations between nearby protons. The peak identification from the starting materials, PGA and Fol-PEG, were compared to the generated polymers and confirmed with HSQC.

Poly-L-α-glutamic acid:

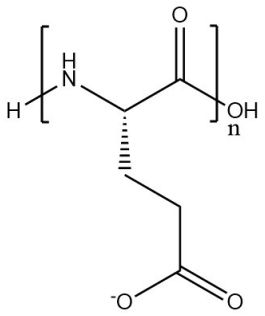

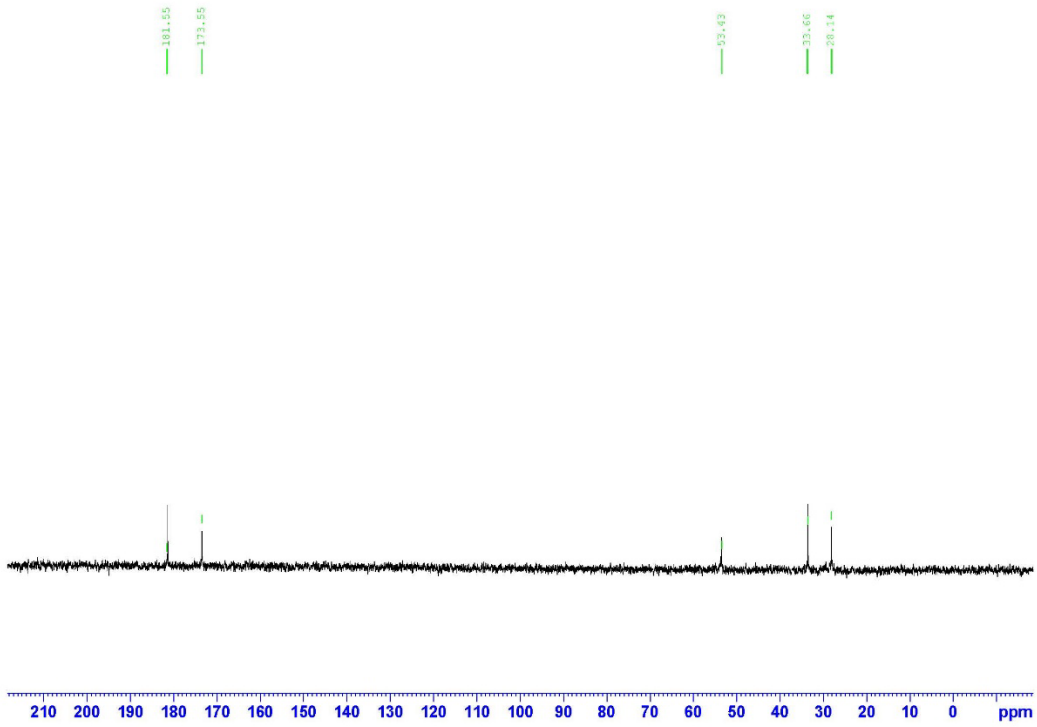

Figure 22: ^{13}C spectra for PGA (32 scans)

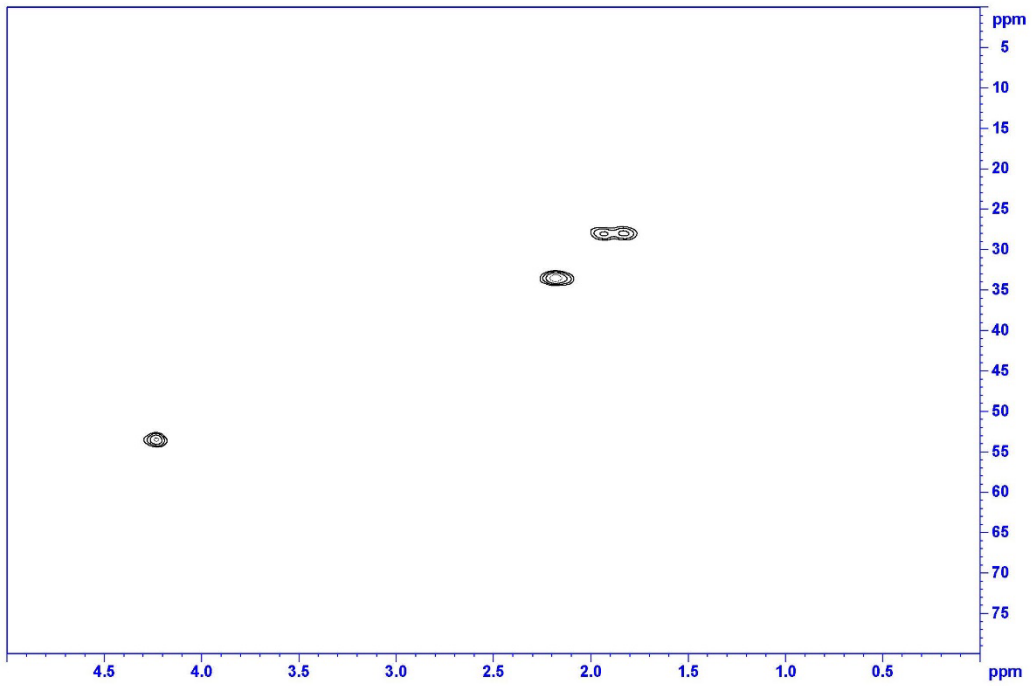

Figure 23: HSQC spectra for PGA (32 scans)

NMR for PGA was collected in D_2O. ^{13}C NMR was simply identified using known ^{13}C chemical shifts for glutamic acid. Using known values, the α-carbon was at 53.43 ppm, β-carbon at 28.14 ppm, and γ-carbon at 33.66 ppm. Further out, the side chain carboxylate was at 181.55 ppm and the backbone amide carbon was at 173.55 ppm. These collected values were consistent with standard values.

^{13}C HSQC was used to identify the α-, β-, and γ- protons associated with the α-, β-, and γ-carbons. Using the above ^{13}C spectra as reference, the α-proton was located at 4.2 ppm, the β-protons were at 1.9 ppm, and the γ-protons were at 2.2 ppm. These chemical shifts remain consistent with standard values.

Folate-PEG600-NH_2

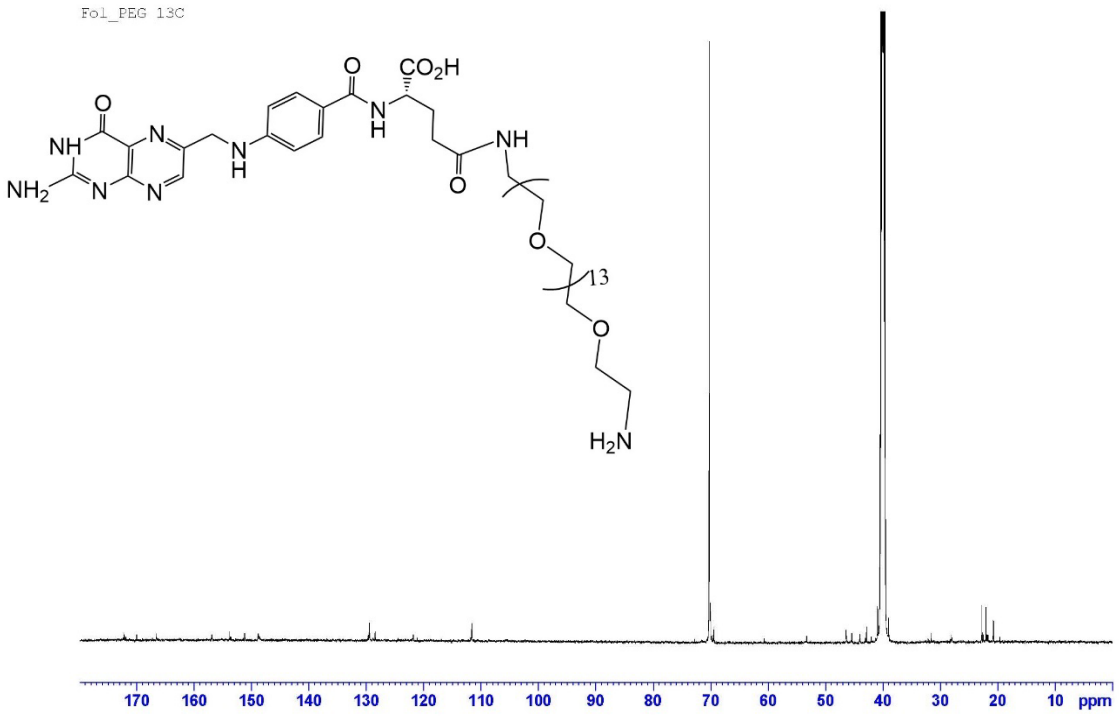

Figure 24: ^{13}C spectra for Folate-PEG600-NH_2 (2000 scans)

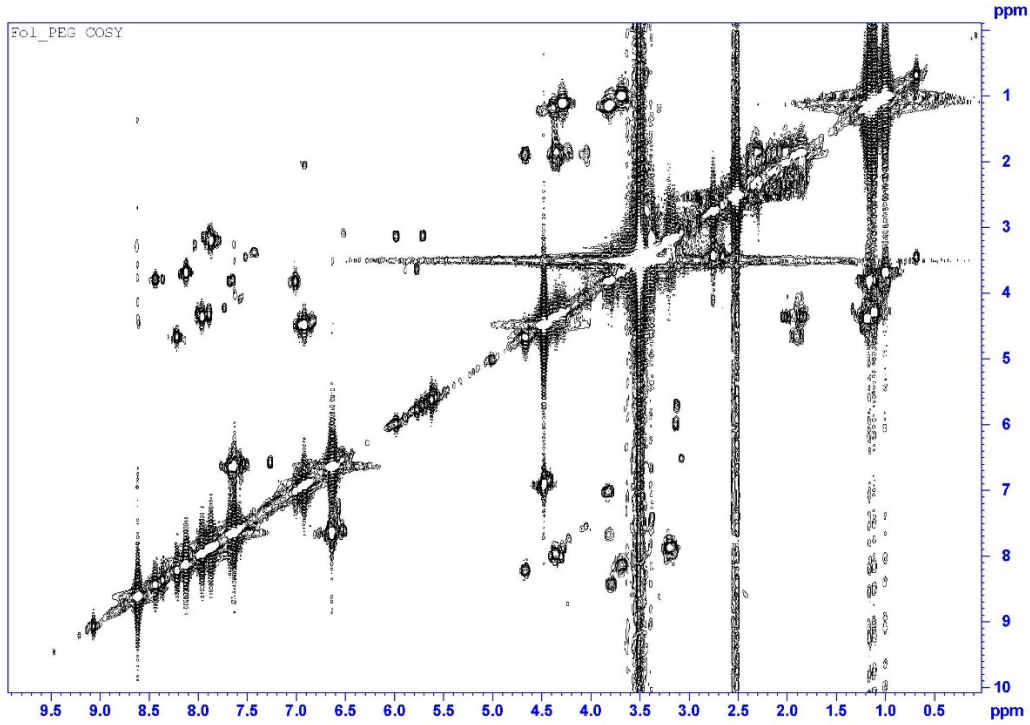

Figure 25: COSY spectra for Folate-PEG600-NH_2 (8 scans)

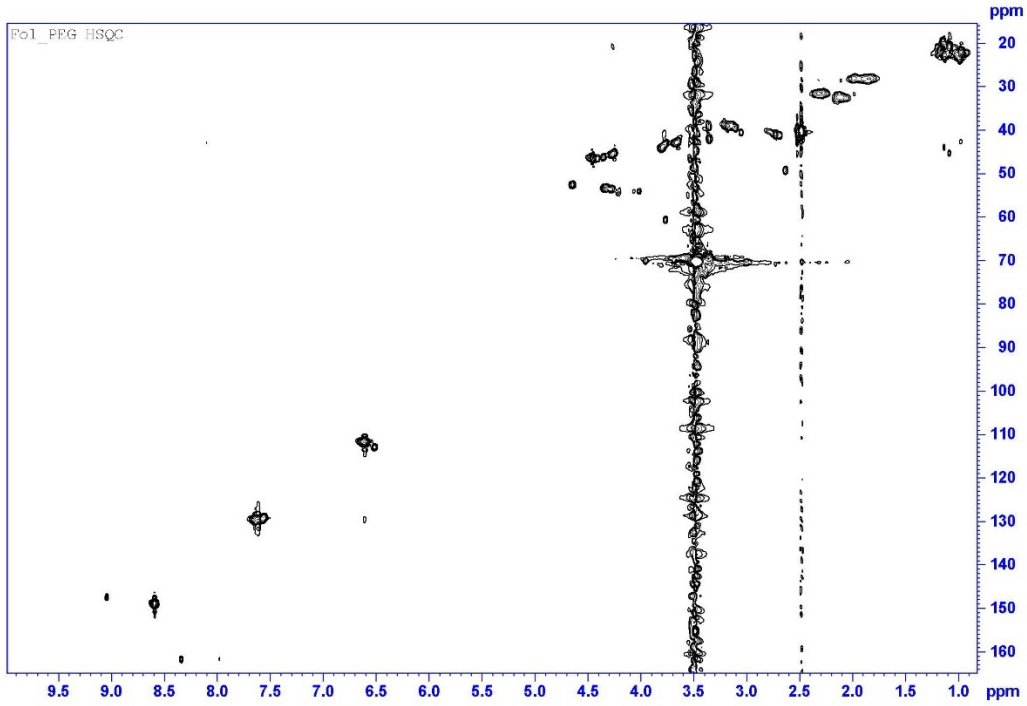

Figure 26: HSQC spectra for Folate-PEG600-NH_2 (8 scans)

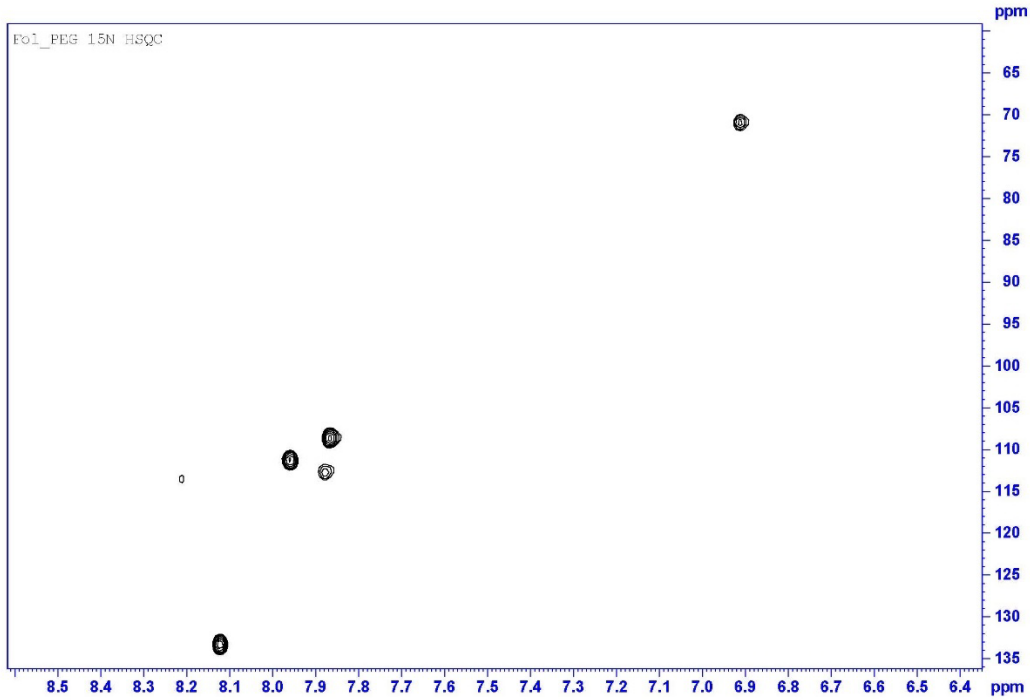

Figure 27: ^{15}N HSQC spectra for Folate-PEG600-NH_2 (16 scans)

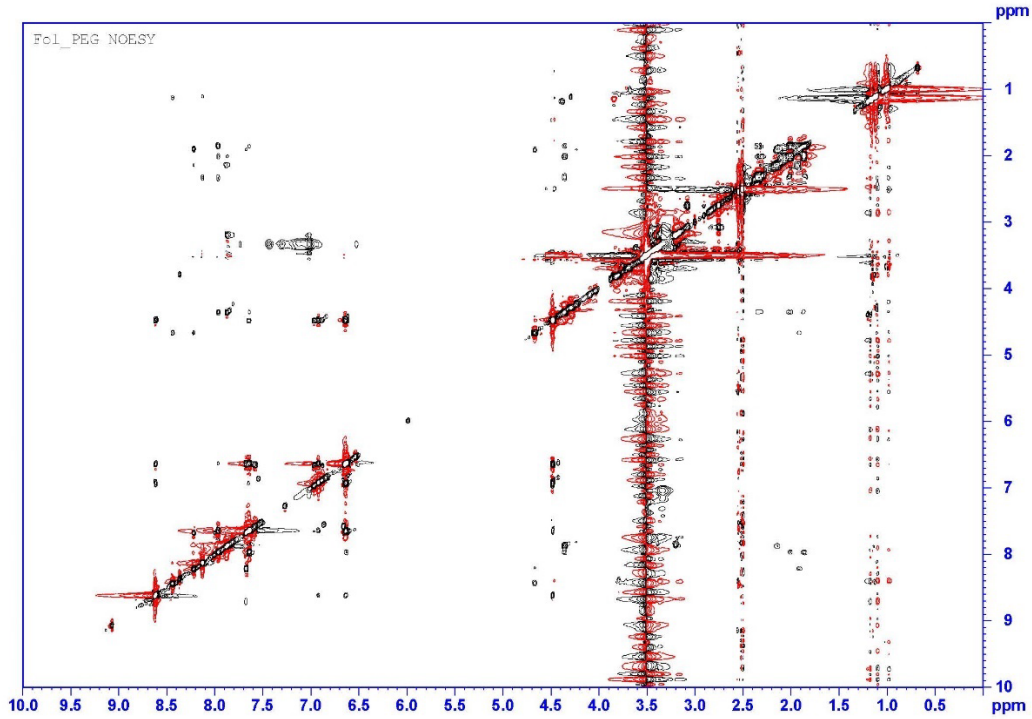

Figure 28: NOESY spectra for Folate-PEG600-NH_2 (16 scans)

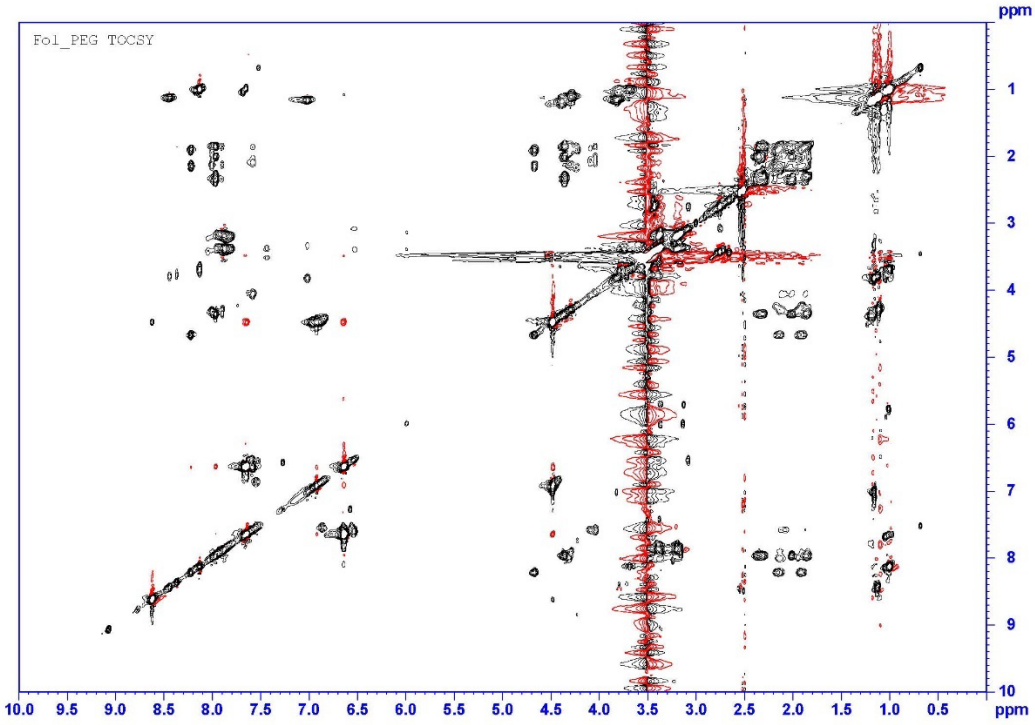

Figure 29: TOCSY spectra for Folate-PEG600-NH_2 (16 scans)

NMR spectra for Fol-PEG was collected in DMSO-d6. The ^{13}C NMR of the Folate-PEG starting material clearly identifies the DMSO solvent at 40 ppm and the PEG carbons at 70 ppm. The ^{13}C spectrum (Figure 24) in combination with ^{13}C-HSQC (Figure 26) suggests that the carbons around 20 ppm and the protons around 1 ppm are nonrelated peaks to the molecule as they only intersect with themselves and the solvent. Additionally, TOCSY, COSY, and NOESY show that these non-associated protons interact with nearly every other proton, suggesting a contamination or peaks associated with the sample tube itself. The carbon HSQC (Figure 26) is most beneficial in identifying the fingerprint aromatic protons at 6.6 ppm, 7.6 ppm and 8.6 ppm along with their associated carbons at 112 ppm, 129.5 ppm, and 149 ppm, respectively. These easily identified protons were primarily used to confirm folic acid's presence in the tagged polymers. In addition, many of the nitrogen-associated protons are clearly identified in the ^{15}N-HSQC (Figure 27) at 6.9 ppm, 7.8 ppm, 7.9 ppm, 8.1 ppm, and 8.2 ppm. COSY and TOCSY (Figures 25 and 29, respectively) show the proximity of some of these fingerprint protons, with 6.6 ppm and 7.6 ppm being closely correlated, consistent with their assignments as the aromatic ring protons. Additionally, the amine proton at 6.9 ppm correlates with the protons at 4.5 ppm, consistent with their assignments as the bridge between the pteridine ring and the aromatic ring.

PGA-Fol(1)

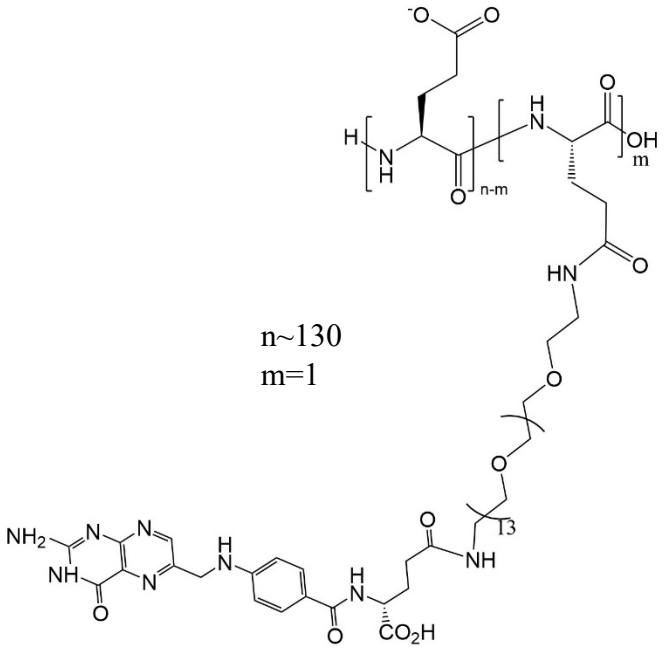

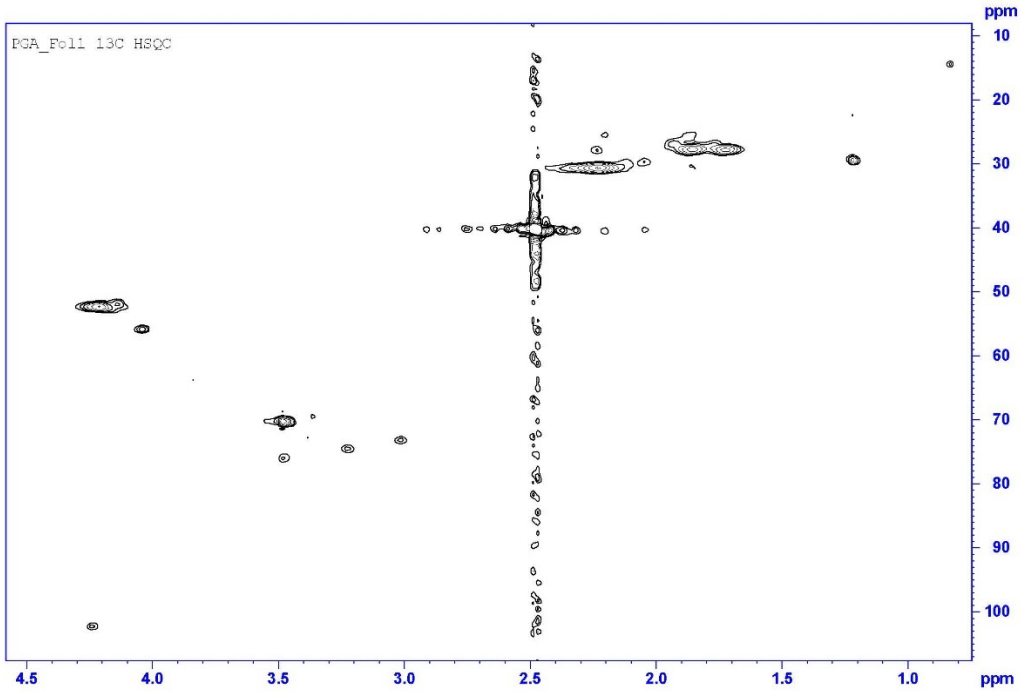

Figure 30: HSQC for PGA-Fol(1) (16 scans)

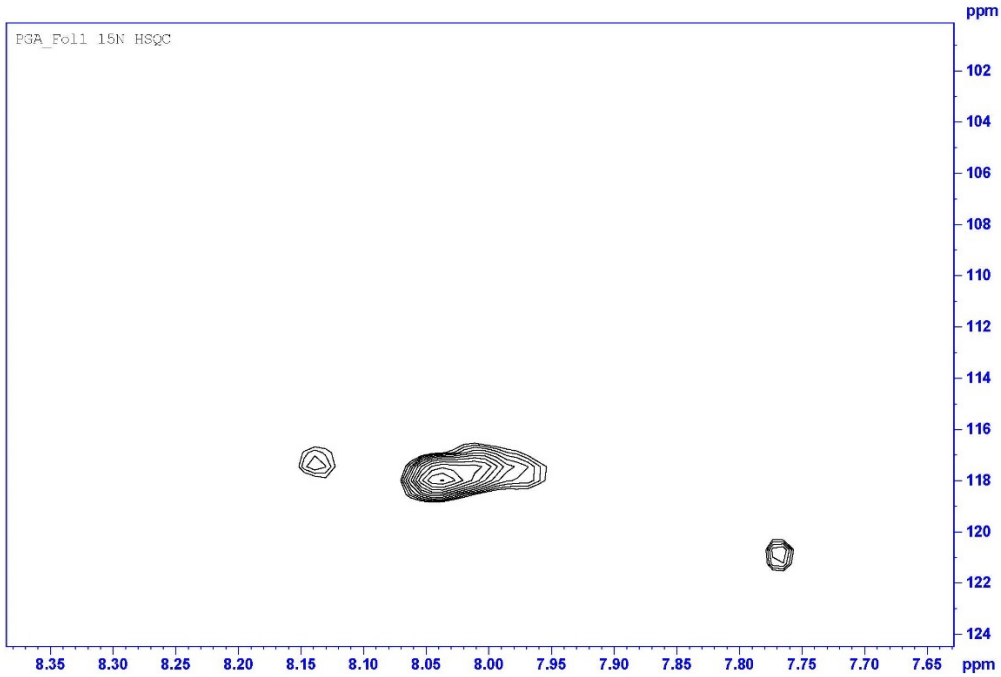

Figure 31: ^{15}N HSQC for PGA-Fol(1) (32 scans)

NMR for PGA-Fol(1) was collected in a 90:10 (v:v) H_2O:D_2O mixture. Proton peak identification was primarily performed through comparison with PGA and Folate-PEG starting materials. The two methods of HSQC were utilized to confirm assignments from the starting material confirmation. ^{15}N-HSQC confirms the presence of the nitrogen-associated protons at 7.7 ppm, 8.0 ppm, and 8.1 ppm (Figure 31). The lack of clear peaks for all nitrogen-associated protons is likely a combination of the D_2O suppression in addition to the conformation of the polymer hiding some of the expected peaks. The ^{13}C-HSQC (Figure 30) confirms the presence of the PGA-associated protons at 4.2 ppm (α-carbon), 1.9 ppm (β-carbon), and 2.2 ppm (γ-carbon).

PGA-Fol(3)

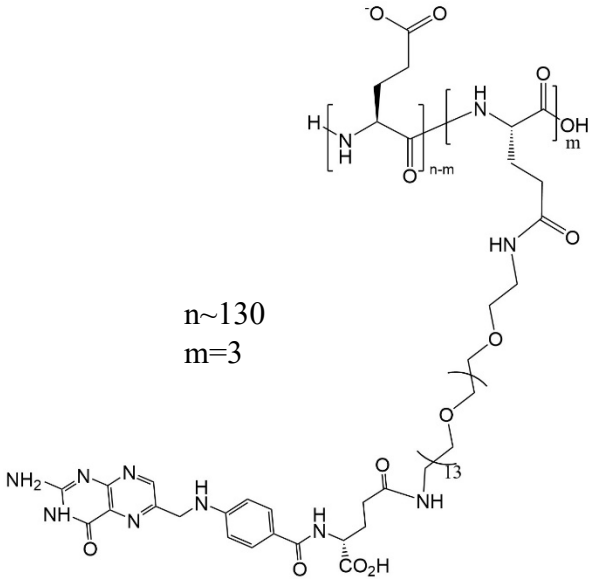

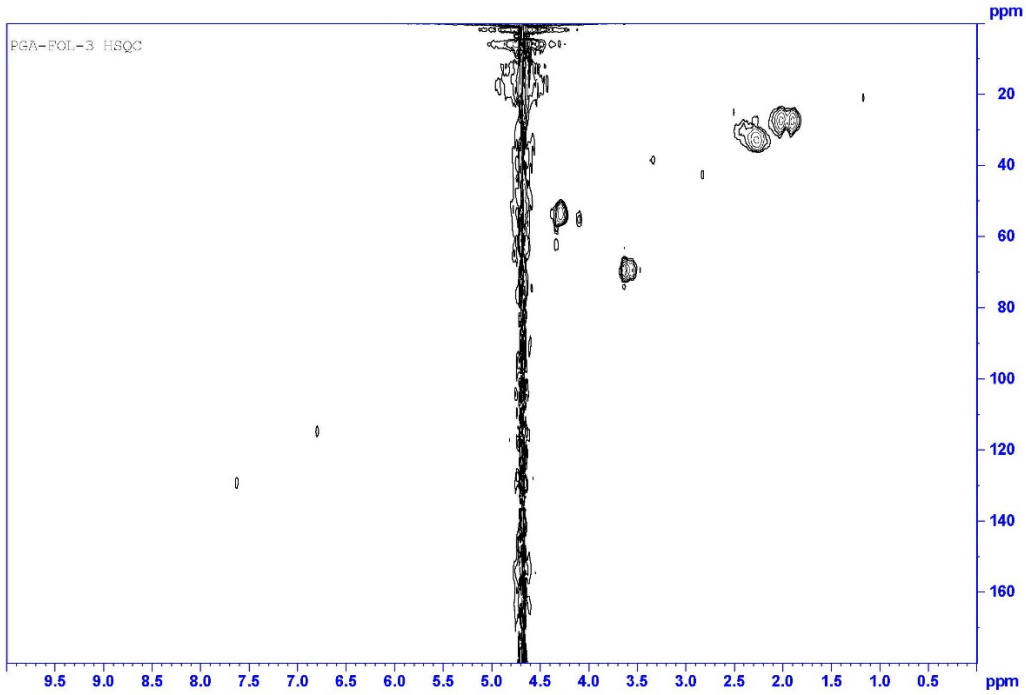

Figure 32: HSQC for PGA-Fol(3) (64 scans)

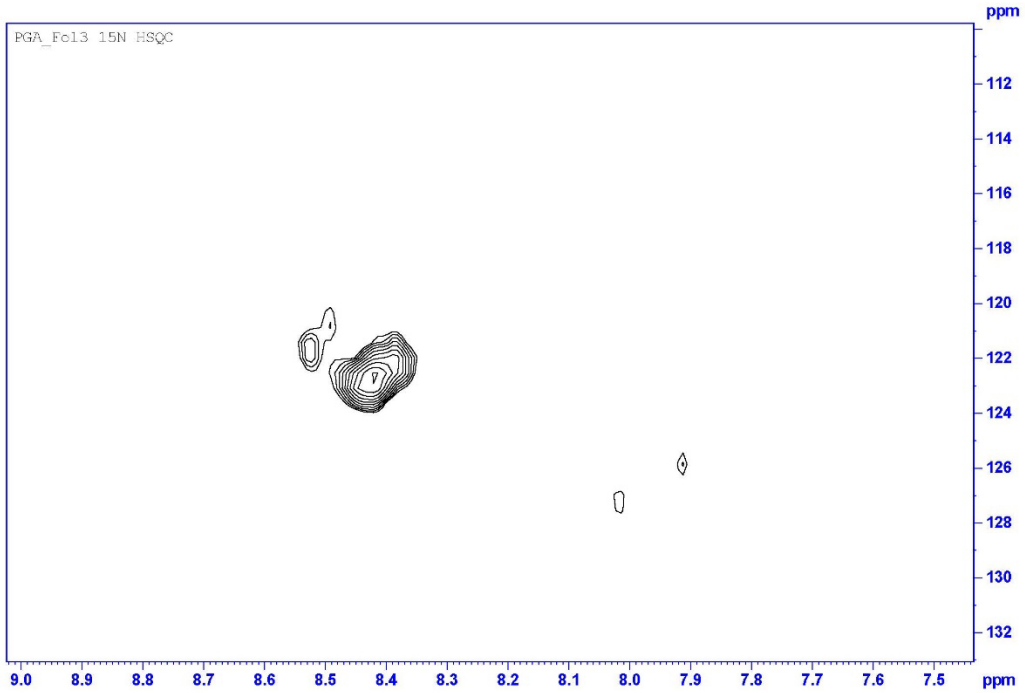

Figure 33: ^{15}N HSQC for PGA-Fol(3) (128 scans)

NMR for PGA-Fol(3) was collected in a 90:10 (v:v) H_2O:D_2O mixture. Proton peak identification was primarily performed through comparison with PGA and Folate-PEG starting materials. The two methods of HSQC were utilized to confirm assignments from the starting material confirmation. ^{15}N-HSQC confirms the presence of the amide protons at 7.7 ppm, 8.4 ppm, and 8.5 ppm (Figure 33). The lack of clear peaks for all nitrogen-associated protons is likely a combination of the D_2O suppression in addition to the conformation of the polymer hiding some of the expected peaks. The ^{13}C-HSQC (Figure 32) confirms the presence of the PGA-associated protons at 4.2 ppm (α-carbon), 1.9 ppm (β-carbon), and 2.2 ppm (γ-carbon).

PGA-Fol(7)

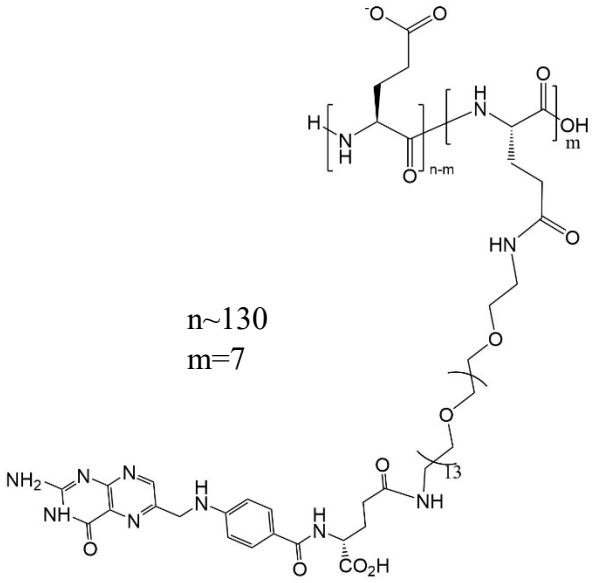

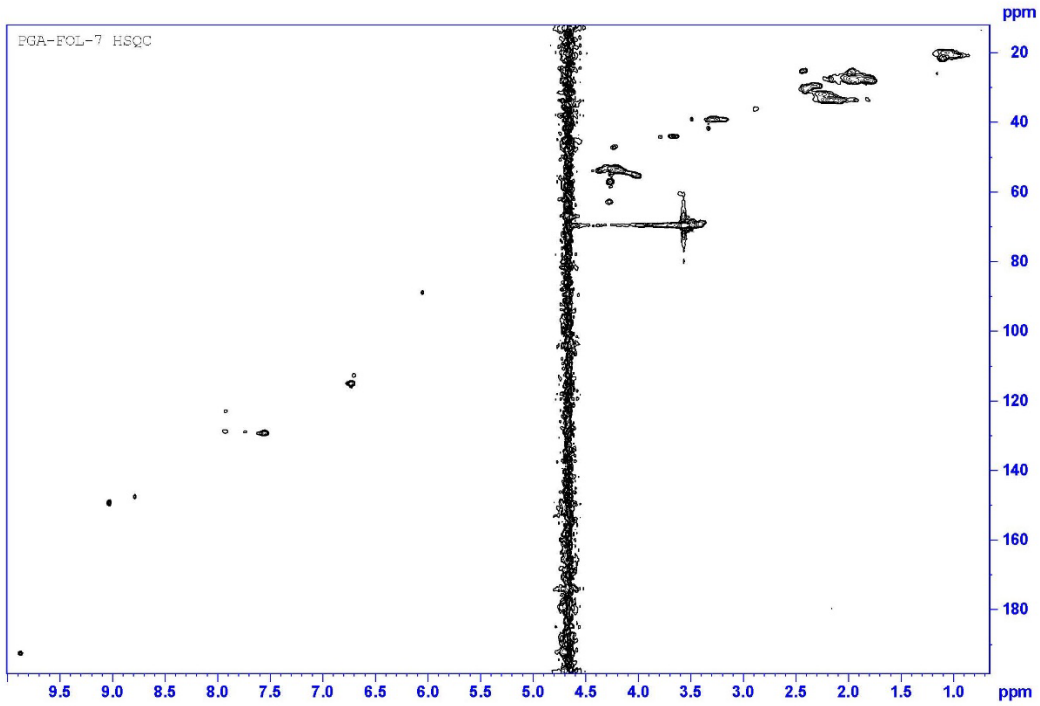

Figure 34: HSQC for PGA-Fol(7) (16 scans)

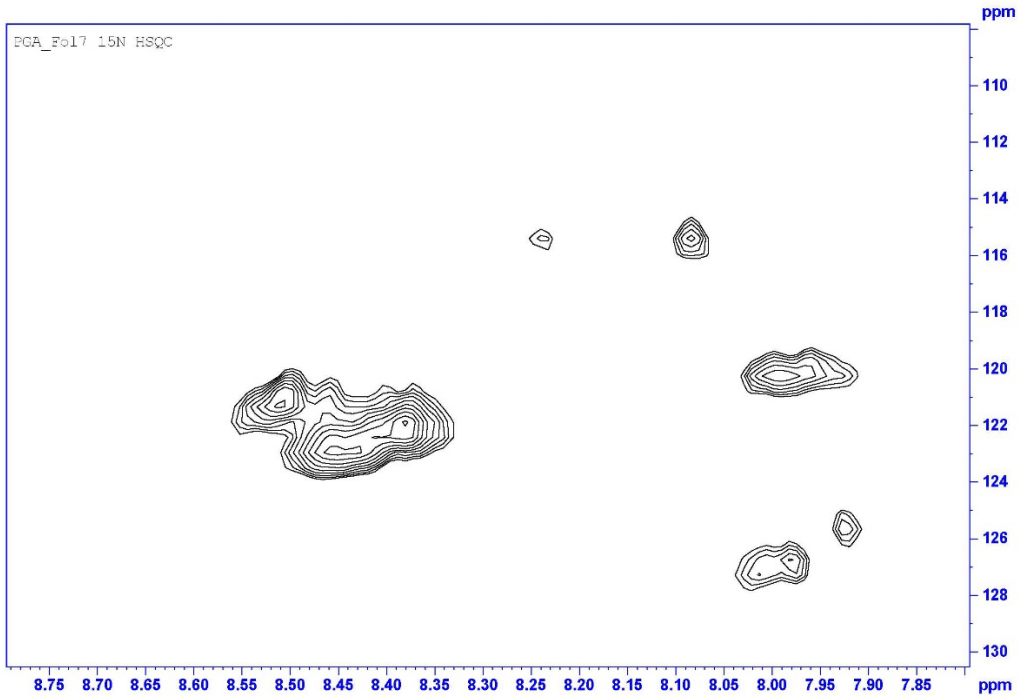

Figure 35: ^{15}N HSQC for PGA-Fol(7) (64 scans)

NMR for PGA-Fol(7) was collected in a 90:10 (v:v) H_2O:D_2O mixture. Proton peak identification was primarily performed through comparison with PGA and Folate-PEG starting materials. The two methods of HSQC were utilized to confirm assignments from the starting material confirmation. ^{15}N-HSQC confirms the presence of the amide protons at 7.9 ppm, 8.0 ppm, 8.4 ppm, and 8.5 ppm (Figure 35). The ^{13}C-HSQC (Figure 34) confirms the presence of the PGA-associated protons at 4.2 ppm (α-carbon), 1.9 ppm (β-carbon), and 2.2 ppm (γ-carbon). In addition, the later aromatic protons reappear, suggesting that the conformation-associated peak loss has decreased. For example, the aromatic ring peaks at 6.6 ppm and 7.6 ppm have reappeared with PGA-Fol(7).

LIST OF REFERENCES

1. Pack, D.W., et al., *Design and development of polymers for gene delivery.* Nat Rev Drug Discov, 2005. **4**(7): p. 581-93.
2. Gautam, P., et al., *Promoter optimisation of lentiviral vectors for efficient insulin gene expression in canine mesenchymal stromal cells: potential surrogate beta cells.* J Gene Med, 2016. **18**(10): p. 312-321.
3. Ghosh, R. and S.J. Tabrizi, *Gene suppression approaches to neurodegeneration.* Alzheimers Res Ther, 2017. **9**(1): p. 82.
4. Michaelsen, S.R., et al., *Single agent- and combination treatment with two targeted suicide gene therapy systems is effective in chemoresistant small cell lung cancer cells.* Journal of Gene Medicine, 2012. **14**(7): p. 445-458.
5. Blaese, R.M., et al., *T lymphocyte-directed gene therapy for ADA- SCID: initial trial results after 4 years.* Science, 1995. **270**(5235): p. 475-80.
6. LTD, J.W.a.S. *Gene Therapy Clinical Trials Databases*. Gene Therapy Clinical Trials Worldwide 2022 January 28, 2023]; Available from: http://www.genetherapynet.com/clinical-trials.html
7. Research, C.f.B.E.a. *Approved Cellular and Gene Therapy Products*. 2022 [cited 2023; Available from: https://www.fda.gov/vaccines-blood-biologics/cellular-gene-therapy-products/approved-cellular-and-gene-therapy-products
8. Medina-Kauwe, L.K., J. Xie, and S. Hamm-Alvarez, *Intracellular trafficking of nonviral vectors.* Gene Ther, 2005. **12**(24): p. 1734-51.
9. Kumari, S., S. Mg, and S. Mayor, *Endocytosis unplugged: multiple ways to enter the cell.* Cell Res, 2010. **20**(3): p. 256-75.
10. Khalil, I.A., et al., *Uptake pathways and subsequent intracellular trafficking in nonviral gene delivery.* Pharmacol Rev, 2006. **58**(1): p. 32-45.
11. Pei, J., et al., *Targeting Lysosomal Degradation Pathways: New Strategies and Techniques for Drug Discovery.* J Med Chem, 2021. **64**(7): p. 3493-3507.
12. Rejman, J., et al., *Size-dependent internalization of particles via the pathways of clathrin- and caveolae-mediated endocytosis.* Biochem J, 2004. **377**(Pt 1): p. 159-69.
13. Doherty, G.J. and H.T. McMahon, *Mechanisms of endocytosis.* Annu Rev Biochem, 2009. **78**: p. 857-902.
14. Recouvreux, M.V. and C. Commisso, *Macropinocytosis: A Metabolic Adaptation to Nutrient Stress in Cancer.* Front Endocrinol (Lausanne), 2017. **8**: p. 261.
15. Ferraro, B., et al., *Clinical applications of DNA vaccines: current progress.* Clin Infect Dis, 2011. **53**(3): p. 296-302.

16. Diehl, W.E., et al., *Tracking interspecies transmission and long-term evolution of an ancient retrovirus using the genomes of modern mammals.* Elife, 2016. **5**: p. e12704.

17. Lundstrom, K., *Viral Vectors in Gene Therapy.* Diseases, 2018. **6**(2).

18. Robbins, P.D., H. Tahara, and S.C. Ghivizzani, *Viral vectors for gene therapy.* Trends Biotechnol, 1998. **16**(1): p. 35-40.

19. Cui, J., T.E. Schlub, and E.C. Holmes, *An allometric relationship between the genome length and virion volume of viruses.* J Virol, 2014. **88**(11): p. 6403-10.

20. Mali, S., *Delivery systems for gene therapy.* Indian J Hum Genet, 2013. **19**(1): p. 3-8.

21. Li, C., et al., *Adeno-associated virus vectors: potential applications for cancer gene therapy.* Cancer Gene Ther, 2005. **12**(12): p. 913-25.

22. Huser, D., et al., *Integration preferences of wildtype AAV-2 for consensus rep-binding sites at numerous loci in the human genome.* PLoS Pathog, 2010. **6**(7): p. e1000985.

23. Weber, T., *Anti-AAV Antibodies in AAV Gene Therapy: Current Challenges and Possible Solutions.* Front Immunol, 2021. **12**: p. 658399.

24. Milone, M.C. and U. O'Doherty, *Clinical use of lentiviral vectors.* Leukemia, 2018. **32**(7): p. 1529-1541.

25. Ramamoorth, M. and A. Narvekar, *Non viral vectors in gene therapy- an overview.* J Clin Diagn Res, 2015. **9**(1): p. GE01-6.

26. Felgner, P.L., et al., *Lipofection: a highly efficient, lipid-mediated DNA-transfection procedure.* Proc Natl Acad Sci U S A, 1987. **84**(21): p. 7413-7.

27. Godbey, W.T. and A.G. Mikos, *Recent progress in gene delivery using non-viral transfer complexes.* J Control Release, 2001. **72**(1-3): p. 115-25.

28. Cardarelli, F., et al., *The intracellular trafficking mechanism of Lipofectamine-based transfection reagents and its implication for gene delivery.* Sci Rep, 2016. **6**: p. 25879.

29. Pollard, H., et al., *Polyethylenimine but not cationic lipids promotes transgene delivery to the nucleus in mammalian cells.* J Biol Chem, 1998. **273**(13): p. 7507-11.

30. Godbey, W.T., K.K. Wu, and A.G. Mikos, *Poly(ethylenimine) and its role in gene delivery.* J Control Release, 1999. **60**(2-3): p. 149-60.

31. Behr, J.P., *The proton sponge: A trick to enter cells the viruses did not exploit.* Chimia, 1997. **51**(1-2): p. 34-36.

32. Wagner, E. and J. Kloeckner, *Gene delivery using polymer therapeutics.* Polymer Therapeutics I: Polymers as Drugs, Conjugates and Gene Delivery Systems, 2006. **192**: p. 135-173.

33. Haensler, J. and F.C. Szoka, *Polyamidoamine Cascade Polymers Mediate Efficient Transfection of Cells in Culture.* Bioconjugate Chemistry, 1993. **4**(5): p. 372-379.

34. Amoozgar, Z. and Y. Yeo, *Recent advances in stealth coating of nanoparticle drug delivery systems.* Wiley Interdiscip Rev Nanomed Nanobiotechnol, 2012. **4**(2): p. 219-33.

35. Shi, B., et al., *Challenges in DNA Delivery and Recent Advances in Multifunctional Polymeric DNA Delivery Systems.* Biomacromolecules, 2017. **18**(8): p. 2231-2246.

36. Dash, P.R., et al., *Factors affecting blood clearance and in vivo distribution of polyelectrolyte complexes for gene delivery.* Gene Ther, 1999. **6**(4): p. 643-50.

37. Ernsting, M.J., et al., *Factors controlling the pharmacokinetics, biodistribution and intratumoral penetration of nanoparticles.* J Control Release, 2013. **172**(3): p. 782-94.

38. Kurosaki, T., et al., *Ternary complexes of pDNA, polyethylenimine, and gamma-polyglutamic acid for gene delivery systems.* Biomaterials, 2009. **30**(14): p. 2846-53.

39. Mott, L., *Effect of Surface Charge on Polyplex Internalization and Intracellular Trafficking.* Journal of Drug Delivery Science and Technology, 2023.

40. Hamada, E., et al., *Anionic Complex with Efficient Expression and Good Safety Profile for mRNA Delivery.* Pharmaceutics, 2021. **13**(1).

41. Gabrielson, N.P. and D.W. Pack, *Efficient polyethylenimine-mediated gene delivery proceeds via a caveolar pathway in HeLa cells.* J Control Release, 2009. **136**(1): p. 54-61.

42. Moghimi, S.M., et al., *A two-stage poly(ethylenimine)-mediated cytotoxicity: implications for gene transfer/therapy.* Mol Ther, 2005. **11**(6): p. 990-5.

43. Sabin, J., et al., *New insights on the mechanism of polyethylenimine transfection and their implications on gene therapy and DNA vaccines.* Colloids and Surfaces B-Biointerfaces, 2022. **210**.

44. Zwicke, G.L., G.A. Mansoori, and C.J. Jeffery, *Utilizing the folate receptor for active targeting of cancer nanotherapeutics.* Nano Rev, 2012. **3**.

45. Kelemen, L.E., *The role of folate receptor alpha in cancer development, progression and treatment: cause, consequence or innocent bystander?* Int J Cancer, 2006. **119**(2): p. 243-50.

46. Toffoli, G., et al., *Expression of folate binding protein as a prognostic factor for response to platinum-containing chemotherapy and survival in human ovarian cancer.* Int J Cancer, 1998. **79**(2): p. 121-6.

47. Yoo, H.S. and T.G. Park, *Folate-receptor-targeted delivery of doxorubicin nano-aggregates stabilized by doxorubicin-PEG-folate conjugate.* J Control Release, 2004. **100**(2): p. 247-56.

48. Yin, M., et al., *Water-dispersible multiwalled carbon nanotube/iron oxide hybrids as contrast agents for cellular magnetic resonance imaging.* Carbon, 2012. **50**(6): p. 2162-2170.

49. Rajagopalan, P.T., et al., *Interaction of dihydrofolate reductase with methotrexate: ensemble and single-molecule kinetics.* Proc Natl Acad Sci U S A, 2002. **99**(21): p. 13481-6.

50. Richter, F., et al., *The impact of anionic polymers on gene delivery: how composition and assembly help evading the toxicity-efficiency dilemma.* Journal of Nanobiotechnology, 2021. **19**(1).

51. Norton, N., et al., *Folate receptor alpha expression associates with improved disease-free survival in triple negative breast cancer patients.* NPJ Breast Cancer, 2020. **6**: p. 4.

52. Batys, P., et al., *pH-Induced Changes in Polypeptide Conformation: Force-Field Comparison with Experimental Validation.* J Phys Chem B, 2020. **124**(14): p. 2961-2972.

53. Atlas, T.H.P. *Cell Atlas- FOLR1*. 2022 [cited 2023; Available from: www.proteinatlas.org/ENSG00000110195-FOLR1/cell.

54. Bandara, N.A., M.J. Hansen, and P.S. Low, *Effect of receptor occupancy on folate receptor internalization.* Mol Pharm, 2014. **11**(3): p. 1007-13.

55. Lajoie, P. and I.R. Nabi, *Lipid Rafts, Caveolae, and Their Endocytosis.* International Review of Cell and Molecular Biology, Vol 282, 2010. **282**: p. 135-163.

56. Miller, C.R., et al., *Liposome-cell interactions in vitro: effect of liposome surface charge on the binding and endocytosis of conventional and sterically stabilized liposomes.* Biochemistry, 1998. **37**(37): p. 12875-83.

57. Gratton, S.E., et al., *The effect of particle design on cellular internalization pathways.* Proc Natl Acad Sci U S A, 2008. **105**(33): p. 11613-8.

58. Sigismund, S., et al., *Clathrin-mediated internalization is essential for sustained EGFR signaling but dispensable for degradation.* Developmental Cell, 2008. **15**(2): p. 209-219.

59. Islam, M.M., I. Hlushchenko, and S.G. Pfisterer, *Low-Density Lipoprotein Internalization, Degradation and Receptor Recycling Along Membrane Contact Sites.* Frontiers in Cell and Developmental Biology, 2022. **10**.

60. Cao, M.Z., et al., *Folic acid directly modified low molecular weight of polyethyleneimine for targeted pDNA delivery.* Journal of Drug Delivery Science and Technology, 2020. **56**.

61. Dutta, D. and J.G. Donaldson, *Search for inhibitors of endocytosis: Intended specificity and unintended consequences.* Cell Logist, 2012. **2**(4): p. 203-208.

62. Ivanov, A.I., *Pharmacological inhibition of endocytic pathways: is it specific enough to be useful?* Methods Mol Biol, 2008. **440**: p. 15-33.

63. Lubyphelps, K., et al., *Hindered Diffusion of Inert Tracer Particles in the Cytoplasm of Mouse 3t3 Cells.* Proceedings of the National Academy of Sciences of the United States of America, 1987. **84**(14): p. 4910-4913.

64. Drake, D.M. and D.W. Pack, *Biochemical investigation of active intracellular transport of polymeric gene-delivery vectors.* Journal of Pharmaceutical Sciences, 2008. **97**(4): p. 1399-1413.

65. Lu, Y., et al., *An Overview of Tubulin Inhibitors That Interact with the Colchicine Binding Site.* Pharmaceutical Research, 2012. **29**(11): p. 2943-2971.

66. Mukhtar, E., V.M. Adhami, and H. Mukhtar, *Targeting Microtubules by Natural Agents for Cancer Therapy.* Molecular Cancer Therapeutics, 2014. **13**(2): p. 275-284.

67. Casella, J.F., M.D. Flanagan, and S. Lin, *Cytochalasin-D Inhibits Actin Polymerization and Induces Depolymerization of Actin-Filaments Formed during Platelet Shape Change.* Nature, 1981. **293**(5830): p. 302-305.

68. Kobayashi, T., et al., *Inhibition of Dynein Atpase by Vanadate, and Its Possible Use as a Probe for Role of Dynein in Cytoplasmic Motility.* Biochemical and Biophysical Research Communications, 1978. **81**(4): p. 1313-1318.

69. Beckerle, M.C. and K.R. Porter, *Inhibitors of Dynein Activity Block Intracellular-Transport in Erythrophores.* Nature, 1982. **295**(5851): p. 701-703.

70. Hopkins, S.C., R.D. Vale, and I.D. Kuntz, *Inhibitors of kinesin activity from structure-based computer screening.* Biochemistry, 2000. **39**(10): p. 2805-2814.

71. Subramanian, R. and J. Gelles, *Two distinct modes of processive kinesin movement in mixtures of ATP and AMP-PNP.* Journal of General Physiology, 2007. **130**(5): p. 445-455.

72. Wang, L. and R.C. MacDonald, *Effects of microtubule-depolymerizing agents on the transfection of cultured vascular smooth muscle cells: Enhanced expression with free drug and especially with drug-gene lipoplexes.* Molecular Therapy, 2004. **9**(5): p. 729-737.

73. Suh, J., D. Wirtz, and J. Hanes, *Efficient active transport of gene nanocarriers to the cell nucleus.* Proceedings of the National Academy of Sciences of the United States of America, 2003. **100**(7): p. 3878-3882.

CALEB AKERS VITA

Education

B.A. Biochemistry and Physics, DePauw University, May 2017

Ph.D. Pharmaceutical Sciences, University of Kentucky, August 2023

Professional Positions

Graduate Research Assistant, University of Kentucky Department of Pharmaceutical Sciences, Lexington, KY, August 2017- May 2023

Honors and Awards

Dennis Casey Pharmaceutical Chemistry and Engineering Graduate Student Travel Award, 2019

Pharmaceutical Sciences Graduate Student Recruitment Fellowship Award, 2018

Peer Reviewed Publications

Landon Mott, **Caleb Akers**, Daniel W. Pack. "Effect of polyplex surface charge on cellular internalization and intracellular trafficking" *Journal of Drug Delivery Science and Technology*, vol. 84, 2023, https://doi.org/10.1016/j.jddst.2023.104465.

Fitzgerald, Gracie, et al. "Controlled Release of DNA Binding Anticancer Drugs from Gold Nanoparticles with near-Infrared Radiation." *Journal of Pharmaceutical Sciences*, 7 Dec. 2022, https://doi.org/10.1016/j.xphs.2022.12.001.

Nardo, David, **Akers, Caleb M**, et al. "Cyanuric Chloride as the Basis for Compositionally Diverse Lipids." *RSC Advances*, vol. 11, no. 40, 15 July 2021, pp. 24752–24761., https://doi.org/10.1039/d1ra02425f.

Hale, Jacob, and **Caleb Akers**. "Deceleration of Droplets That Glide along the Free Surface of a Bath." *Journal of Fluid Mechanics* 803 (2016): 313-31

Akers, Caleb Michael, Nathaniel John Smith, and Naima Shifa. "Multinomial Logistic Regression Model for Predicting Tornado Intensity Based on Path Length and Width." *World Environment* 4.2 (2014): 61-66.

Oral Presentations

Folate Receptor-Targeted Anionic Ternary Polyplexes for Gene Delivery- Presented as an oral presentation at American Institute of Chemical Engineers National Conference in Nov 2019, Orlando, FL

Improving Therapeutic Options via Bionanotechnology- Presented as a poster at American Chemical Society National Meeting in April 2017, San Francisco, CA

Deceleration of droplets that glide along the free surface of a bath- Presented as a poster at American Physical Society Division of Fluid Dynamics conference in Nov. 2014, San Francisco, CA